Laser spark in gases

G. V. Ostrovskaya and A. N. Zaĭdel'

A. F. Ioffe Physico-technical Institute, USSR Academy of Sciences

Usp. Fiz. Nauk **111**, 579–615 (December 1973)

A survey is presented of papers published from 1964 through 1971 on the laser spark in gases. The authors consider the mechanisms whereby laser radiation breaks down a gas, the influence of the experimental conditions on the breakdown threshold, and the interaction of the spark plasma with the laser radiation. The parameters of the plasma during the time it is acted upon by the radiation and after the end of the laser pulse are determined. The possibilities of a number of technical applications of a laser spark in gases are discussed.

CONTENTS

1. INTRODUCTION

When the radiation of a sufficiently powerful laser is focused on the surface of a solid target or in a volume filled with gas, a hot and dense plasma is produced. Interest in this plasma is due both to the desire to obtain record high temperatures (up to thermonuclear) and electron densities, and the possibility of observing a large number of very interesting phenomena connected with the interaction of high-intensity radiation with a plasma. We consider here only research on the plasma produced when laser radiation is focused in a gas. This plasma is called in the literature "laser spark."

The first to report observation of gas breakdown by a laser beam was Maker in 1963[1]. A detailed analysis of the theoretical and experimental work performed up to the middle of 1965 is contained in the review by Raĭzer[2]. Whereas at the time of its publication the total number of papers devoted to breakdown of gases by lasers was approximately 40, by now the number of publications has exceeded 400. (A bibliography and a survey of work performed until 1968 can be found in[3]). The first papers presented the basic concepts of the mechanism whereby breakdown is produced and of the interaction of laser radiation with a plasma. Many theoretical and experimental papers were subsequently devoted to a more detailed analysis of these processes. At the same time, in conjunction with progress in laser techniques, gas breakdown by laser radiation was investigated between continuously increasing experimental limits. While in the first studies the laser spark was obtained with pulses from ruby ($\lambda = 0.6943\ \mu$) and neodymium ($\lambda = 1.06\ \mu$) lasers lasting several dozen nanoseconds, at the present time laser sparks are obtained by using radiation of wavelength from $0.26\ \mu$ (fourth harmonic of neodymium laser) to $10.6\ \mu$ (CO_2 laser). A laser spark is obtained with pulses lasting from several picoseconds to several milliseconds; high-power cw lasers are also used to maintain the plasma.

The expansion of the range of the experimental conditions under which gas breakdown by laser radiation is investigated has not only contributed to a deeper understanding of the mechanism whereby radiation interacts with gases and with plasma, but has also made it possible to observe a number of new phenomena, particularly the self-focusing of the laser radiation during the breakdown process.

The present review covers papers published through the end of 1971. Greatest attention is paid to researches following the publication of Raĭzer's review[2].

2. GAS BREAKDOWN UNDER THE INFLUENCE OF LASER RADIATION

a) Breakdown threshold. When the radiation intensity exceeds a certain threshold value, breakdown is produced in the gas and is accompanied by absorption of an appreciable fraction of the laser-pulse energy and formation of a highly-ionized hot plasma. The breakdown is accompanied by a bright flash and a characteristic sound recalling a spark discharge. The breakdown threshold depends on the type of gas and its pressure, on the radiation wavelength, on the duration of the laser pulse, and on the condition of its focusing.

The breakdown threshold is usually characterized by the threshold density I_{thr} of the light flux or by the threshold density $F_{thr} = I_{thr}/h\nu$ of the photon flux, and also by the critical electric field intensity $E_{thr} = (4\pi I_{thr}/c)^{1/2}$ (c is the speed of light). If I_{thr} is measured in W/cm^2 and E_{thr} in V/cm, then the connection between E_{thr} and I_{thr} can be written in the form $E_{thr} = 19(I_{thr})^{1/2}$.

In the case of ruby-laser pulses of duration of several dozen nanoseconds, the breakdown thresholds of most gases at pressures close to atmospheric are on the order of 10^{29}–10^{30} photons/cm^2sec (10^{10}–10^{11} W/cm^2).

The abrupt increase of the absorption of laser radiation by the gas is the result of its ionization in the field of the light wave. There are two processes that can explain the ionization due to focusing of an intense light beam in a gas, namely multiphoton ionization and cascade ionization. The first process can occur independently of the presence of free electrons in the focal region, whereas cascade ionization must be initiated by at least one priming electron.

b) Multiphoton ionization. Since the ionization energy of most gases ranges from 10 to 20 eV, which is much larger than the energy of one ruby- or neodymium-laser

emission quantum (1.78 and 1.18 eV, respectively), ionization of the atoms calls for simultaneous absorption of several quanta. This process has been named multiphoton ionization. The ionization of an atom in the field of an intense light wave can be considered also as a direct detachment of an electron from the atom by the alternating electric field.

The theory of multiphoton ionization has been the subject of a large number of papers (see, e.g., [4-14]). Without dwelling on an exposition, we present the principal relations characterizing the dependence of the multiphoton ionization threshold on the experimental conditions.

The number of quanta necessary to ionize an atom is obviously

$$n = \left\langle \frac{U_i}{h\nu} + 1 \right\rangle, \tag{1}$$

where U_i is the ionization energy, $h\nu$ is the quantum energy, and $\langle \ldots \rangle$ denotes the integer part of the quantity contained in the brackets. The probability of simultaneous absorption of n quanta is proportional to the light flux raised to the n-th power

$$w = AF^n. \tag{2}$$

The total number N_e of ionization acts is proportional to the atom concentration n_a, to the duration Δt of the laser pulse, and to the volume V of the focal zone:

$$N_e = An_a \Delta t\, VF^n. \tag{3}$$

Assuming that the breakdown occurs when a certain critical value $N_{e,cr}$ is reached, we obtain for the threshold photon-flux density

$$F_{thr} = \left(\frac{N_{e,cr}}{An_a \Delta t\, V} \right)^{1/n}. \tag{4}$$

Thus, F_{thr} depends relatively little on the initial gas density, on the duration of the laser pulse, or on the dimensions of the focal region.

Detailed quantum-mechanical calculations of the probability of multiphoton ionization with allowance for not only the initial and final energy states of the atom, but also of the intermediate states, were performed by Gold and Bebb[7,8]. They have shown that the ionization energy increases abruptly if the excitation energy of one of the intermediate states is close to the energy of an integer number of quanta ($E_{exc} = mh\nu$). According to the calculated data given in[7,8], at near-atmospheric pressure and at a ruby-laser pulse duration $\approx$10 nsec, the threshold breakdown powers due to multiphoton ionization amount in the case of hydrogen and inert gases to $10^{30}-10^{32}$ photons/cm^{2}sec, which is larger by one or two orders of magnitude than the measured breakdown thresholds. At the same time, the fluxes needed to detach one electron in the focal volume coincide in order of magnitude with the experimentally measured breakdown thresholds. Thus, under these conditions multiphoton ionization can cause only the appearance of the initial priming electrons. The number of electrons is further increased as a result of cascade ionization.

The weak dependence of the threshold flux on the gas density ($F_{thr} \sim n_a^{1/n}$) causes even a negligible concentration of easily-ionized impurities to lead to the appearance of priming electrons. Thus, multiphoton ionization of the residual gas in a vacuum chamber was observed directly in[15]. At a pressure 10^{-6} mm Hg, several dozen electrons were produced during the time of the pulse.

To observe multiphoton processes in pure form, it is necessary to exclude cascade-ionization processes. To this end it suffices to decrease the gas pressure to values such that the mean free path of the electrons exceeds the dimensions of the focal volume. The laser spark is not produced in this case, but an appreciable number of ions is produced, and by measuring this number it is possible to estimate experimentally the probability of the multiphoton processes. Investigations of this kind were carried out in[16-22].

In accord with (3), the number of produced ions ($N_i \approx N_e$) is proportional to F^n. From the slope of the plot of the function $\log N_i = f(\log F)$ we can determine the number n of simultaneously absorbed quanta. In all cases, the experimentally measured number n_{exp} turns out to be smaller by several units than the number determined by formula (1). The decrease in the number of quanta necessary for the ionization can be due to the smearing of the upper levels of the atom in strong electromagnetic fields[23]. A similar effect can result from the smearing of intermediate levels, which increases the probability of quasiresonant transitions[24].

c) Cascade ionization. The primary electrons produced as a result of multiphoton ionization absorb the light quanta in collisions with neutral atoms. The energy of the electron increases to values exceeding somewhat the ionization energy. After this, the electron ionizes the atom, with a high probability, as a result of which two electrons appear, and the process is repeated. The number of electrons increases exponentially:

$$N_t = N_0 e^{\gamma t} = N_0 2^{t/\tau}; \tag{5}$$

here $\gamma = (1/\tau)\ln 2$ is the cascade-development constant and τ is the time necessary to double the number of electrons.

The final number of electrons depends very strongly on the cascade development constant, which in turn depends on the electromagnetic field intensity. This explains why the process has a threshold character. The breakdown threshold is determined from the condition that during the time Δt of the pulse the total number of electrons must reach a certain critical value N_{cr}. Then

$$\gamma_{cr} = \frac{1}{\Delta t} \ln \frac{N_{cr}}{N_0} \tag{6}$$

The theory of cascade ionization is the subject of[25-35]. Without stopping to discuss these studies (an analysis of the work performed up to 1965 is given in Raĭzer's review[2]), we present the basic relations characterizing the cascade-ionization process.

The growth rate of the electron energy in the electromagnetic field of the radiation is given by

$$\frac{d\varepsilon}{dt} = \frac{e^2E^2}{m} \frac{\nu_{eff}}{\omega^2 + \nu_{eff}^2} \approx \frac{4\pi e^2}{mc} \frac{\nu_{eff}}{\omega^2 + \nu_{eff}^2} I; \tag{7}$$

Here $\nu_{eff} = n_a v \sigma_{tr}$ is the effective collision frequency, n_a is the concentration of the atoms, v is the electron velocity, σ_{tr} is the transport cross section, e and m are the charge and mass of the electron, E and ω are the intensity and frequency of the field, and I is the density of the light flux. At not too high gas densities, when $\nu_{eff} \ll \omega$, we have

$$\frac{d\varepsilon}{dt}=\frac{4\pi e^2}{mc}\frac{\nu_{eff}}{\omega^2}I. \quad (8)$$

The time τ necessary to double the number of electrons can be determined from the condition that during that time the electron acquires an energy equal to the ionization energy of the atom:

$$U_i=\int_0^\tau \frac{d\varepsilon}{dt}dt\approx\frac{4\pi e^2}{mc}\frac{\nu_{eff}}{\omega^2}I\tau, \quad (9)$$

whence

$$\gamma=\frac{4\pi(\ln 2)e^2\nu_{eff}I}{mcU_i\omega^2}. \quad (10)$$

The threshold intensity is obtained by equating the value of γ from (10) to γ_{cr} (6):

$$I_{thr}=\frac{mcU_i\omega^2\ln(N_{cr}/N_0)}{4\pi(\ln 2)e^2n_a v\sigma_{tr}\Delta t}. \quad (11)$$

For ruby-laser pulses of nanosecond duration, the calculated values of the threshold intensities are in reasonable agreement with the experimental values of the breakdown thresholds.

It should be noted that the growth rate of the cascade can decrease as a result of energy losses by the electron via elastic and inelastic collisions, and also as a result of diffusion of the electrons from the focal region and recombination processes.

Inelastic collisions that lead to excitation of atoms can either slow down or accelerate the cascade development. In strong optical fields, the excited atoms and molecules are ionized with high probability, and this leads to acceleration of the cascade development[28,29]. In fields of lower intensity, however, the atoms lose the excitation energy by radiation. The role of these losses is particularly appreciable in the breakdown of gases by long-wave radiation (for example, by neodymium-laser and CO_2-laser radiation). Allowance for losses of this type leads to the appearance of an additional factor in Eq. (10), corresponding to the probability that the electron will pass through the excitation region[25]. The question of the role of excitation of vibrational levels in the breakdown of molecular gases is considered in[35]. Allowance for the deceleration of the electrons by vibration levels leads to a weaker dependence of the breakdown threshold on the pressure and on the laser-pulse duration than given by (11).

Calculations of cascade ionization with allowance for diffusion and recombination losses are carried out in[30,31,36,37]. The growth of the electron concentration is described in this case by the equation

$$\frac{\partial n_e}{\partial t}=(\gamma-\gamma_a)n_e+D\nabla^2n_e-\alpha_R n_e^2, \quad (12)$$

where n_e is the electron concentration, D is the diffusion coefficient, α_R is the recombination coefficient, γ is the ionization constant connected with the density of the light flux by relation (10), and γ_a characterizes the losses to "sticking" (a process in which the electron and atom form a negative ion). At relatively low pressures, when the principal role is played by diffusion losses, the solution of (12) for the case of a cylindrical focal volume and for a laser pulse of triangular wave form yields the following expression for the threshold intensity

$$I_{thr}=C\left(\frac{1}{\Delta t}\ln\frac{N_{cr}}{N_0}+\frac{2D}{\Lambda^2}\right), \quad (13)$$

where

$$C=\frac{mcU_i\omega^2}{4\pi(\ln 2)e^2n_a v\sigma_{tr}},$$

Δt is the duration at half-height, and Λ is the characteristic diffusion length, which is connected with the length l and the diameter d of the cylindrical focal volume by the relation $1/\Lambda^2=(\pi/l)^2+(4.8/d)^2$. Neglecting diffusion, we can obtain from (13) the previously derived expression (11) for the breakdown threshold. In the case of small focal volumes and low pressures (large D), the breakdown threshold is determined mainly by the diffusion losses.

It has been assumed so far that the electron constantly acquires energy and then ionizes the atom practically instantaneously at the instant when its energy reaches the atom's ionization energy. In gas breakdown by powerful ultrashort pulses, the character of the cascade development changes. In this case the energy acquired by the electron in one elastic collision, which is of the order of the energy of the oscillations of the electron in the field of the light wave, can exceed the atoms ionization energy. The electron then rapidly enters an energy region in which the ionization probability decreases with increasing electron energy. As a result, the cascade development constant does not increase but decreases with increasing laser-radiation intensity. The theory of cascade ionization under the influence of powerful ultrashort pulses was developed by Afanas'ev and others[32-34].

A comparison of expressions (4) and (11) for the gas breakdown thresholds governed by the multiphoton and cascade-ionization processes shows that the threshold radiation densities with these two processes depend differently on the laser pulse duration, on the dimensions of the focal region, and on the pressure and ionization potential of the gas. The investigation of the dependence of the breakdown threshold on the experimental conditions is therefore of considerable interest when it comes to ascertaining the breakdown mechanism.

d) Pressure dependence of breakdown threshold. The pressure dependence of the breakdown threshold was investigated in[31,36-42]. For pressures close to atmospheric and for laser pulses of nanosecond duration, the breakdown threshold is seen to decrease with increasing pressure. A typical plot of I_{thr} against pressure is shown for inert gases in Fig. 1. The slope of the $\log I_{thr} = f(\log p)$ plots is close to unity, in agreement with the theory of cascade ionization, as is typical of an inverse proportionality of the breakdown threshold to the pressure (see formula (11)). For molecular gases, the slope

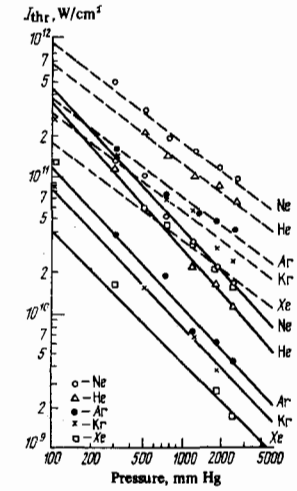

FIG. 1. Pressure dependence of breakdown threshold for inert gases (solid lines—neodymium laser, dashed—ruby) [41].

of the plot of $\log I_{thr}$ against $\log p$ is somewhat smaller[41].

With increasing pressure, the slope of the plots decreases, and at pressures on the order of hundreds of atmospheres a minimum is observed on the curves[36,39,40] (Fig. 2). The existence of this minimum was predicted by Minck[38]. Indeed, according to (7) the growth rate of the electron energy has a maximum at $\omega = \gamma_{eff} = n_a v \sigma_{tr}$, so that the breakdown threshold should have a minimum at an atom concentration $n_a \approx \omega/v\sigma_{tr}$.

It should also be noted that the change of pressure can lead to a significant change in the magnitude and character of the electron energy loss, which in turn should affect the rate of cascade development. Thus, the decrease in the slope of the plot of $\log I_{thr}$ against $\log p$ with increasing pressure can be due to the enhanced role of the recombination processes[31,37]. The decrease of the pressure leads to an increase in the diffusion coefficient (see formula (13)) and to a corresponding increase in the diffusion losses.

e) Dependence of the breakdown threshold on the sort of gas. Both ionization mechanisms—multiphoton and cascade—lead to an appreciable dependence of the breakdown threshold on the gas ionization potential. An experimentally clear-cut dependence of the breakdown threshold on the ionization potential was observed for inert gases[41,43]. As seen from Fig. 3, the breakdown threshold increases sharply when the ionization potential increases. The only exceptions are neon and helium, for in spite of the large ionization potential helium has a lower breakdown threshold. The same picture is observed when the breakdown of these gases is produced by a ruby or neodymium laser, and can therefore not be attributed to resonance effects. In addition, the closest to resonance (in the case of the ruby-laser emission quanta) is the energy of one of the Ne-atom levels, and this could lead to a decrease rather than an increase of the breakdown threshold of Ne in comparison with He.

The dependence of the breakdown threshold on the ionization potential is not so pronounced for molecular gases as for inert gases[41-43]. A comparison of the thresholds is made difficult in this case by the different slopes of the plots of $\log I_{thr}$ against $\log p$ for different gases, so that the form of the dependence of the breakdown threshold on the ionization potential is determined essentially by the pressure.

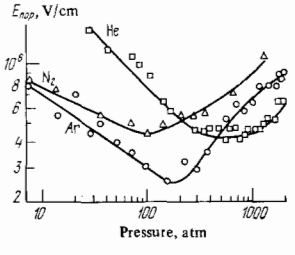

FIG. 2. Pressure dependence of breakdown threshold [39].

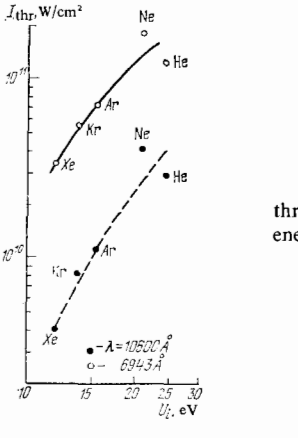

FIG. 3. Dependence of the breakdown threshold of inert gases on the ionization energy ($p = 10^3$ mm Hg) [41].

There have been several investigations of the influence of impurity on the breakdown threshold. Thus, it is shown in[44] that addition of freon to argon can lead, depending on the experimental conditions, to either an increase or a decrease of the breakdown threshold. For comparatively low pressures (≈ 250 mm Hg), the breakdown threshold was lowered by the addition of freon, and in the opinion of the authors, was due to multiphoton ionization of the freon, which provided the priming electrons. At high pressures (≈ 2500 mm Hg), and at slowly rising pulses, addition of the freon leads to the capture of the free electrons and hinders the cascade development, thus leading to an increase in the breakdown threshold.

A curious phenomenon was observed by Smith and Haught[45]. A small addition of neon ($\approx 1\%$) to argon leads to an appreciable lowering of the threshold of breakdown by neodymium-laser radiation as compared with the breakdown threshold in pure argon (we recall that the breakdown threshold in neon is higher than in argon). A more detailed investigation of breakdown in argon-neon mixtures was made by Mul'chenko and Raĭzer[46]. They observed a sharp decrease of the breakdown threshold at the neodymium-laser frequency not only with small amounts of Ne in Ar, but also with small amounts of Ar in Ne. In the latter case this can be attributed to the Penning effect (acceleration of cascade development as a result of ionization of argon atoms in collisions with excited neon atoms). However, the reason for the lower threshold in argon with a small amount of neon added remains unexplained. No such effect is observed in the breakdown of neon-argon mixture by ruby-laser radiation. The difference in the character of the dependence of the breakdown threshold on the mixture composition for neodymium and ruby lasers is due, in the opinion of Mul'chenko and Raĭzer[46], to the different role of the photoionization of excited atoms during the process of cascade development: the photoionization of the excited atoms by ruby-laser radiation is much more rapid than in the case of a neodymium laser, when the photoionization calls for a larger number of quanta. Therefore the Penning effect hardly comes into play in the breakdown by ruby-laser radiation.

f) Dependence of the breakdown threshold on the radiation frequency. The dependence of the breakdown threshold on the wavelength of the laser radiation was investigated in[40,41,47-51]. In the first papers[40,41,47] the breakdown thresholds were compared at two frequencies (neodymium laser ($\lambda = 1.06\ \mu$) and its harmonic $\lambda = 0.53\ \mu$[47], and neodymium and ruby ($\lambda = 0.69\ \mu$) lasers[40,41]). In both cases, the breakdown threshold for the longer-wavelength radiation of the neodymium laser was much lower than for the shorter-wavelength ruby laser or for the harmonic of the neodymium laser, this being in qualitative agreement with the relation $I_{thr} \sim \omega^2$ predicted by the cascade-ionization theory for the frequency dependence of the breakdown threshold. However, a comparison of the breakdown threshold by using more than two wavelengths, carried out in[48-51], has shown that the dependence of I_{thr} on the wavelength is

not monotonic. Buscher et al.[48] measured the breakdown thresholds in inert gases at the neodymium (1.06 μ) and ruby (0.69 μ) frequencies, and their second harmonics (0.53 and 0.35 μ). A maximum of the threshold breakdown power was observed, with a position that depended on the nature of the gas (Fig. 4).

The dependence of the breakdown threshold on the wavelength was investigated in[49,51] using a neodymium laser and its second, third, and fourth harmonics (0.53, 0.35, and 0.26 μ, respectively). A lowering of the breakdown threshold was observed in the ultraviolet region, but this was apparently due both to the increased probability of the multiphoton ionization responsible for the appearance of the priming electrons and for the enhanced role of ionization of the excited states during the course of cascade development.

A more detailed investigation of the dependence of the threshold on the wavelength near the maximum of the $I_{thr} = f(\lambda)$ curve was carried by Alcock et al.[50] using a tunable-frequency dye laser.

Finally, special mention should be made of gas breakdown by long-wave radiation from a pulsed CO_2 laser ($\lambda = 10.6\ \mu$), investigated by Generalov et al.[52] and by Smith[53,54]. The absolute values of the threshold intensities for the breakdown of Ne and He at pressures from 2 to 25 atm, according to the data of[52], were $\approx 10^8$ W/cm^2, which is lower by approximately two orders of magnitude than in the breakdown of these gases by radiation in the visible band. In Smith's studies[53], breakdown was produced by CO_2 radiation only in pre-ionized argon. In this case the absolute values of the breakdown threshold ($\approx 2 \times 10^8$ W/cm^2) were of the same order as in[52], but in the absence of pre-ionization no breakdown was produced even at 10^9 W/cm^2.

g) Dependence of the threshold on the dimensions of the focal volume. The role of diffusion losses in the development of a cascade depends significantly on the dimensions of the focal region (the quantity Λ in formula (13)). Investigations of the dependence of the threshold breakdown on the dimensions of the focal volume are carried out in[31,36,40,45,54-56]. Figure 5 shows typical plots of I_{thr} against the focal length f of the lens.

At relatively low pressures, the experimental plots of I_{thr} against f agree with the calculated ones. However, calculations of diffusion at high pressures (10—100 atm) show that the role of diffusion losses under these conditions should be negligible. Nonetheless, a lowering of the threshold with increasing size of the focal volume was observed also in this case[36,31]. Some authors[36,40,54] have advanced the hypothesis that the dependence of the breakdown threshold on the dimensions of the focal volume may be connected in this case not with the diffusion departure of the electrons, but with other "diffusion-like" processes such as diffusion of the resonant radiation. However, as noted in[46], these processes should not greatly influence the development of the breakdown. In the opinion of the authors of[46], diffusion-like losses are due to true diffusion of the electrons not from the focal volume, but from much smaller regions with maximal field intensity.

h) Dependence of the breakdown threshold on the mode makeup of the laser radiation. When radiation of a multimode laser is focused, the interaction of the different oscillation modes produces at the focus of the lens an interference structure that varies in time and in space; as shown in[57], the radiation intensity at individual points of this structure can exceed by 1—2 orders the mean intensity in the focal volume. When radiation of a single-mode laser is focused, to the contrary, there are no local inhomogeneities in the intensity distribution. The distribution of the field over the focal spot is almost Gaussian[58,59], and its maximum value at the center of the spot is only 1.4 times larger than the average velue of the field.

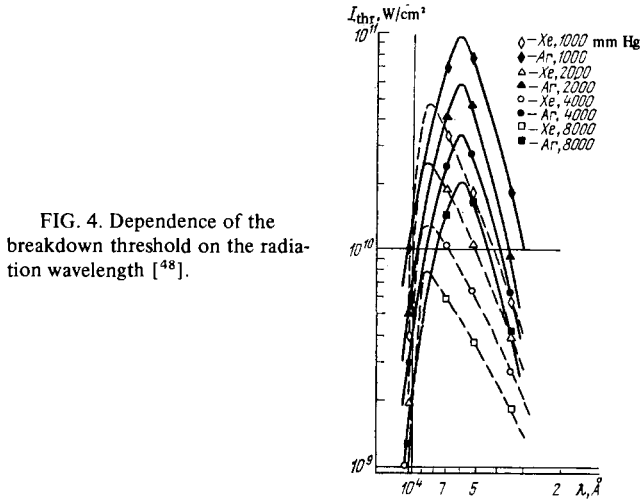

FIG. 4. Dependence of the breakdown threshold on the radiation wavelength [48].

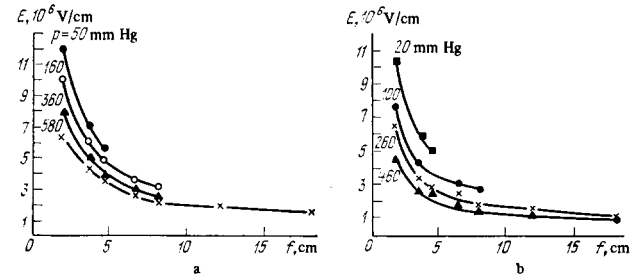

FIG. 5. Dependence of the breakdown threshold on the focal length of the lens [55]. τ_{pulse} = 60 nsec: a) krypton; b) xenon.

Comparisons of the breakdown thresholds using the radiation of single-mode and multimode ruby lasers, carried out by Smith and Tomlinson[58] and by Alcock et al.,[59] have shown that the breakdown thresholds differ insignificantly (the differences do not exceed 50%). The authors have reached the conclusion that under the conditions of their experiments the breakdown occurred under the influence of the field averaged over the focal volume.

i) Dependence of the breakdown threshold on the laser-pulse duration. As seen from (13), in the case of cascade ionization the dependence of the breakdown threshold on the laser-pulse duration is determined essentially by the values of the losses. For short pulses, when $(1/\Delta t)\ln(N_{cr}/N_0) \gg 2D/\Lambda^2$, the diffusion can be neglected and the breakdown threshold is inversely proportional to the pulse length. To the contrary, for long pulses, when $(1/\Delta t)\ln(N_{cr}/N_0) \ll 2D/\Lambda^2$, the breakdown threshold is practically independent of the pulse duration, and for breakdown to occur it is necessary only that the ionization rate exceed the electron losses due to diffusion ($\gamma \geq 2D/\Lambda^2$). The first case corresponds to gas breakdown under the influence of pulses of nanosecond duration. The second case occurs in gas breakdown by

CO_2 laser radiation at pulse durations ≈ 1 μsec and more (see[52]).

The influence of the pulse duration on the breakdown threshold was investigated in[54,60]. The dependence of the breakdown threshold on the pulse duration obtained in[60] (Fig. 6) is in qualitative agreement with the prediction of the theory. The threshold energy density $E_{thr} = I_{thr}\Delta t$ remains constant ($I_{thr} \sim 1/\Delta t$) when the pulse duration changes from 10^{-11} to 10^{-9} sec. In the interval from 10^{-9} to 10^{-7} sec, E_{thr} increases in proportion to Δt, i.e., I_{thr} is constant, corresponding to a high loss level. For a quantitative explanation of this dependence it is necessary to assume, however, that the losses exceed substantially (by almost one order of magnitude) the theoretically calculated value.

k) Gas breakdown by picosecond pulses. Since the breakdown threshold for the cascade ionization mechanism is inversely proportional to the pulse duration, and for multiphoton ionization it depends very weakly on the pulse duration, like $\Delta t^{1/n}$, the breakdowns due to these two processes become comparable in magnitude at picosecond pulse durations. As shown by Bunkin and Prokhorov[61], it becomes possible here to observe gas breakdown as a result of multiphoton ionization in pure form.

To obtain a laser spark, trains of pulses from lasers operating in the mode self-locking regime were used, of $\approx 10^{-11}$ sec duration with intervals of several nanosecond between pulses, as well as individual picosecond pulses separated from such a train and amplified. Even in one of the first studies[58], where the laser spark was produced by a train of picosecond pulses, the question was raised whether the breakdown in this case is the result of the action of an individual picosecond pulse or whether this is cumulative effect due to the entire train and determined by the radiation intensity averaged over the entire pulse train. The authors have concluded, since the average breakdown power (by average power is meant the total energy contained in a train of pulses, divided by the duration of the entire train) of a train of picosecond pulses was equal to that of one pulse of several nanosecond duration, that the breakdown is determined by the averaged action of the entire series of pulses, and not by the instantaneous values of the power, which for individual pulses exceed the average by 2—3 orders of magnitude.

Later investigations[60,62,63], however, have shown that the breakdown is produced by each individual pulse of the train. Alcock et al.[62] have observed that the breakdown threshold does not change when the time intervals between the individual pulses of the train is changed. If the breakdown were to be caused by the action of the entire train, then the diffusion losses during a time between pulses should have led to a growth of the threshold intensity with increasing interval between the pulses. On the other hand, the threshold for breakdown by a single picosecond pulse, measured in[63], were close to the thresholds for the breakdown of the gas by a series of picosecond pulses, as determined in[58]. Finally, Wang and Davis[60] have observed directly that the breakdown produced by individual pulses from a train occurs at discrete points on the laser beam axis and spaced ≈ 0.2 mm apart.

The dependence of the threshold for breakdown under the influence of picosecond pulses on the dimensions of the focal volume was investigated in[64,65]. No dependence of I_{thr} on Λ was observed for a train of picosecond pulses in[64], within the limits of experimental accuracy. (The diffusion losses during the time $\approx 10^{-11}$ sec of one pulse can be neglected.) To the contrary, Bunkin et al.[65] observed a significant dependence of the breakdown threshold on the dimensions of the focal volume. In the opinion of the authors of[65], the possible cause of this dependence is self-focusing of the laser radiation (see Chap. 3 of the present review).

Of particular interest for the elucidation of the mechanism of breakdown under the influence of picosecond pulses is the investigation of the dependence of the breakdown threshold on the pressure[63,66,67]. An appreciable decrease of the breakdown threshold in nitrogen and argon was observed in[63] when the pressure was increased from 500 to 6000 mm Hg, thus offering evidence in favor of the cascade ionization mechanism. A somewhat different dependence of I_{thr} on p was observed by Krasyuk et al.[66,67] (Fig. 7). At a pressure below a certain limit p_0 ($p_0 \approx 5 \times 10^3$ mm Hg for He or Ar and $\approx 4 \times 10^2$ mm Hg for N_2) the value of I_{thr} depends little on the pressure. This region corresponds to multiphoton ionization. The region of higher pressures $p > p_0$ corresponds to cascade ionization. In this case $I_{thr} \sim 1/p$ for He and Ar. The pressure dependence of I_{thr} for N_2 is somewhat weaker, as is typical of cascade ionization of molecular gases.

3. EVOLUTION OF A PLASMA DURING THE TIME IT IS ACTED UPON BY LASER RADIATION

Even in one of the first studies of the laser spark[68] it was observed that after the onset of the primary breakdown the spark develops asymmetrically, namely, the plasma boundary moves towards the focusing lens with a velocity $\approx 10^7$ cm/sec.

A number of mechanisms leading to the motion of the plasma boundary in a direction towards the laser have been considered in the literature. These include the hydrodynamic or detonation mechanism, the breakdown-wave mechanism, the radiation mechanism, and the acceleration of plasma by ponderomotive forces.

The motion of the absorption band in opposition to the light flux hinders the release of the laser-pulse energy into a small volume and imposes a limit on the ability of the laser spark to heat the plasma to high temperatures. This phenomenon was therefore the subject of many theoretical as well as experimental studies.

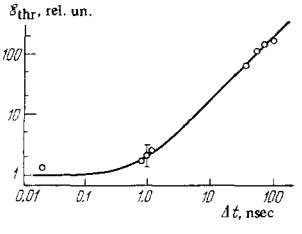

FIG. 6. Dependence of the threshold energy density $\mathcal{E}_{thr} = I_{thr}\Delta t$ on the pulse duration [60].

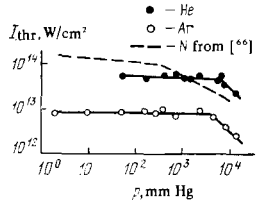

FIG. 7. Pressure dependence of the threshold intensity in gas breakdown by picosecond pulses [67].

a) Hydrodynamic mechanism. The first attempt to explain the propagation of the plasma in a direction opposite to that of the laser radiation was made by Ramsden and Savic[69]. It was assumed that after the breakdown a shock wave propagates through the unperturbed gas, and that further absorption of the energy of the laser pulse occurs behind the shock front moving towards the lens. This mechanism, named the detonation or hydrodynamic mechanism, was considered in greater detail by Raĭzer[2,70]. We confine ourselves here to the presentation of the fundamental relations characterizing this mechanism.

The connection between the velocity v of the detonation wave and the light-flux density I is given by the relation

$$v=\left[2(\gamma^2-1)\frac{I}{\rho_0}\right]^{1/3}, \tag{14}$$

while the internal energy acquired by the gas is equal to

$$\mathscr{E}(T)=\frac{\gamma}{(\gamma^2-1)(\gamma+1)}v^2=\frac{2^{2/3}}{(\gamma^2-1)^{1/3}(\gamma+1)}\left(\frac{I}{\rho_0}\right)^{2/3}; \tag{15}$$

Here γ is the effective adiabatic exponent and ρ_0 is the initial gas density.

Equation (14) gives the instantaneous value of the propagation velocity of the detonation wave. To obtain the law governing the variation of the position of the wave front with time, it is necessary to take into account the fact that the radiation flux I is changed both by the change in the cross section area of the light channel as the detonation wave moves through it, and as a result of the time variation of the radiation power. For a conical light channel we have $I = W(t)/\pi x^2\tan^2\alpha$, where W(t) is the radiation power, x is the distance from the focus of the lens to the wave front, and α is half the angle at the apex of the cone. Substituting the value of I into (14) and replacing v by dx/dt we obtain the differential equation

$$x^{2/3}\frac{dx}{dt}=\left[\frac{2(\gamma^2-1)}{\pi\rho_1\operatorname{tg}^2\alpha}W(t)\right]^{1/3}. \tag{16}$$

In[69] this equation was solved under the assumption that the laser radiation pulse is rectangular, which leads to

$$x=\left(\frac{5}{3}\right)^{3/5}\left[\frac{2(\gamma^2-1)W}{\pi\rho_1\operatorname{tg}^2\alpha}\right]^{1/5}t^{3/5}. \tag{17}$$

Daiber and Thompson[71] considered more realisitc triangular and Gaussian pulses.

It has been assumed so far that the light flux incident on the shock-wave front is completely absorbed in a narrow layer directly adjacent to the front. This takes place if the laser spark is produced in air or in other heavy gases. But if the laser spark is produced in light gases (hydrogen and helium) at relatively low pressures (1–5 atm), then the plasma cannot be regarded as optically dense. The propagation of a detonation wave for this case was also considered by Daiber and Thompson[71]. Formulas (14)–(17) acquire in this case an additional coefficient that accounts for the incomplete absorption of the laser radiation in the shock front.

Lateral expansion causes the absorbed energy to be consumed in heating of a gas volume whose radius exceeds the light-channel radius. The lateral-expansion velocity is close to the sound velocity c in the plasma:

$$c=\sqrt{\gamma(\gamma-1)\mathscr{E}}. \tag{18}$$

Comparing (15) and (18) we get $c/v = \gamma/(\gamma + 1)$, i.e., the velocity of lateral expansion is approximately double the velocity of the detonation wave. As shown in[70], allowance for the lateral expansion leads to replacement of I in formulas (14) and (15) by $I\delta$, where $\delta \approx 1/[1 + (\Delta x/z)]$ is the correction for the lateral expansion, Δx is the thickness of the absorbing zone, approximately equal to the mean free path l of the laser-radiation quanta in the plasma, and r is the radius of the light channel.

The lateral expansion determines, in final analysis, the minimum radiation intensity needed to maintain the detonation regime[72]. In the case when the width of the absorption band is $\Delta x > r$, the energy loss to lateral expansion makes a self-maintaining absorption-wave regime impossible. As shown by Raĭzer[72], much lower radiation intensities are needed to maintain the detonation regime than to break down the gas. Thus, in air at atmospheric pressure $I_{min} \approx 8 \times 10^7$ W/cm^2, and the minimal detonation-wave propagation velocity is $v_{min} \approx 8$ km/sec.

The internal energy determined with the aid of (15) corresponds to a thin layer adjacent to the shock front, in which the radiation energy is released. On the shock-wave front, the gas is compressed to a state with density $\rho_1 = [(\gamma + 1)/(\gamma - 1)]\rho_0$, and then, after acquiring additional energy, expands to a state with density $\rho_2 = [(\gamma + 1)/\gamma]\rho_0$. Behind the high-temperature and high-density gas region adjacent to the detonation-wave front follows a rarefaction region. A shock wave moves also in the opposite direction along the light channel, but the gas temperature is much lower here, since it is assumed that the entire energy is released in a front that propagates towards the laser. The spatial distribution of the plasma parameters of a laser spark for the case of hydrodynamic propagation of the absorption band was considered theoretically in[73–75]. Figure 8 shows the results, obtained by Kidder[75], of numerical calculations of the radial distribution of the plasma parameters when

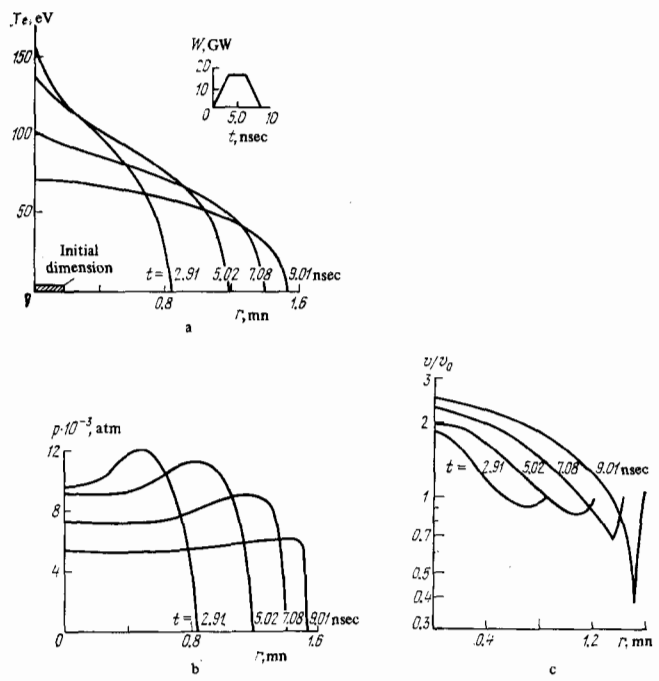

FIG. 8. Radial distribution of the temperature (a), pressure (b), and specific volume (v = 1/ρ) (c) for a laser spark in deuterium (p = 1 atm) in the case of heating by spherically-symmetrical radiation [75]. Pulse energy 100 J, duration 5 nsec; the waveform of the pulse is given in the upper part of Fig. 8a.

the plasma is acted upon by spherically-symmetrical radiation.

b) Breakdown-wave mechanism. If the breakdown in the narrowest part of the light channel occurs before the radiation power has reached the maximum, then with further increase of the power the threshold conditions can be reached also in a broader section of the channel. This leads to a displacement of the breakdown zone in the direction of the lens. The breakdown-wave propagation was considered in[2,70,76-79]. Ambartsumyan et al.[76] have assumed that the breakdown in a given cross section of the light channel occurs at the instant $t = t_{cr}$ when the density of the light flux reaches a certain threshold value I_{cr}. The initial velocity calculated by them for a triangular laser pulse is

$$v(t_{cr}) = \frac{1}{2}\frac{r_0}{t_{cr}\,\mathrm{tg}\,\alpha} = \frac{1}{2}\frac{W_{max}}{\pi r_0 I_{cr}\Delta t\,\mathrm{tg}\,\alpha}\,; \qquad (19)$$

Here w_{max} is the power at the maximum, Δt is the duration at half height, and r_0 is the radius of the channel at the section where the primary breakdown occurs. As seen from (19), the breakdown-wave velocity depends significantly on the power and on the duration of the laser pulse, and also on the focusing lens, which determines the values of $\tan\alpha$ and r_0.

In a paper by Raĭzer[70], published simultaneously with[76], the time necessary for cascade development was taken into account in the calculation of the breakdown-wave propagation velocity. It was assumed that breakdown occurs in a given section of the light channel at the instant when the number of electrons reaches a certain critical value N_{cr}. The formula obtained for the breakdown-wave propagation velocity differed from (19) only by a numerical factor. However, the quantity I_{cr} contained in (19) turns out to be dependent on the wave form of the laser pulse ($I_{cr} \sim \sqrt{W_{max}/\Delta t}$), as a result of which we get

$$v \sim \sqrt{\frac{W_{max}}{\Delta t}}\frac{1}{\mathrm{tg}\,\alpha}\,. \qquad (20)$$

When the breakdown-wave propagation law was derived in[70], it was assumed that the initial electron concentration N_0 is reached in the entire gas volume in which the plasma propagates at the instant when the laser pulse begins. Subsequently Alcock et al.[77,78] performed calculations for the case when the primary electrons appear in a section located at a distance x away from the focus, at a certain time t_1 after the start of the laser pulse (it was assumed that these electrons are produced by ionization of the gas by the radiation of the spark itself). In[79] it was assumed, in the analysis of the motion of the breakdown wave, that the cause of the primary ionization is the laser radiation and that the primary electrons appear in a given cross section when the light flux reaches a certain value I_s sufficient for multiphoton ionization. The initial breakdown-wave velocities obtained in[77,78,79] do not differ from those given by relations (20) and (19) respectively.

c) Radiation mechanism. This mechanism of absorption-zone propagation was considered in detail by Raĭzer[70]. At the temperatures attainable by laser-radiation absorption (10^5–10^6 deg), the mean free path of thermal quanta with energies $h\nu \approx kT$ exceeds not only the width of the absorption wave, but also the dimensions of the heated region. On leaving the plasma, the thermal radiation is absorbed in the adjacent cold layers of the gas, as a result of which the latter are heated to a temperature $\approx 2\times 10^4$ deg and become opaque to the laser radiation. Thus, the laser-radiation absorption zone moves continuously towards the laser.

A rigorous analysis of the radiative transport of the absorption wave is a rather complicated matter. It is shown in[70] that both the dependence of the radiation-wave propagation velocity on the incident light flux and the absolute values of the velocities are approximately the same as for the detonation mechanism.

d) Plasma propagation under the influence of ponderomotive forces. In all the plasma-propagation mechanisms considered so far it was assumed that the interaction between the radiation and the plasma reduces to absorption of light energy and its conversion into thermal energy of the plasma. However, other mechanisms of direct interaction between electromagnetic radiation and a plasma are possible, and lead to its acceleration by nonlinear forces[80-82]. These forces are particular cases of ponderomotive forces. They begin to prevail over the gas dynamic forces if the radiation intensity exceeds a certain critical value I*. For ruby and neodymium lasers, according to the data[80,81], we have $I^* \approx 10^{14}$ W/cm^2. In most experiments on gas breakdown by laser radiation, the intensities are much lower than I*. However, radiation intensities close to I* can be reached within the confines of self-focusing filaments (see below).

e) Experimental investigations of the dynamics of plasma-boundary propagation. The dynamics of the propagation of the plasma boundaries was investigated in[68,69,71,76-79,83-91]. The plasma boundary velocity was determined from scans of the spark radiation, obtained with the aid of image converters[68,71,84,87,88,90], from the Doppler shift of laser radiation scattered by the plasma[83,68,90], and from the time variation of spark contours obtained by the Schlieren method[77,78] and reconstructed with the aid of holograms[85,86].

From a comparison of the results obtained in various papers[68,69,83-86] it follows that the hydrodynamic regime is realized at laser powers from several to several dozen megawatts (the focal lengths of the lenses are several centimeters). In heavy gases, and also in hydrogen and helium at high pressures, the plasma propagated asymmetrically, predominantly towards the laser. In hydrogen and helium at low pressures, two glow fronts were observed, moving in opposite directions (towards the lens and away from it), this being due to the considerable transparency of the laser-spark plasma in these gases.

The initial propagation velocity of the detonation wave in air under normal conditions, measured in[68,71,83,84], ranged from 10^7 to 1.5×10^7 cm/sec.

The good agreement between the measured values of the velocity and the calculated ones[83], the good correspondence between the experimental and theoretical dependences of x on t[69,71], and the approximate two-fold excess of the propagation velocity against the radiation over the lateral velocity[85,86], all indicate that the hydrodynamic plasma-propagation mechanism was realized in these investigations. In addition, the connection between the velocity v and the initial gas density[85] is in good agreement with relation (14). A plot of $v/I^{1/3}$ against $\rho_0^{-1/3}$ is shown in Fig. 9[85]. The points on the plot correspond to laser sparks in air, helium, and hydrogen at different pressures.

The dynamics of plasma expansion under conditions

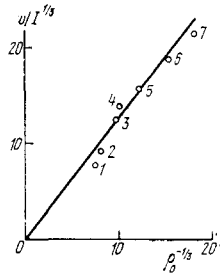

FIG. 9. Dependence of $vI^{1/3}$ on $\rho_0^{-1/3}$ (v is the detonation-wave velocity for t = 10 nsec, I is the light-flux density, and ρ_0 is the initial gas density). 1—Air, 1.75 atm; 2—He, 11 atm; 3—He, 6 atm; 4—H_2, 11 atm; 5—H_2, 6 atm; 6—H_2, 3 atm; 7—H_2, 1.75 atm.

when the breakdown-wave mechanism is realized was investigated in[76-78,87-89]. To obtain a spark, pulses with power from 0.3 to 3 GW were used. In this case, the velocity of the plasma boundary towards the laser greatly exceeded the lateral expansion velocity[76-78]. When the initial gas density was increased, the plasma-boundary propagation velocity increased rather than decreased[76,77,87,88]. The velocities measured in different investigations varied over a wide range, depending on the parameters of the laser pulse and of the focusing lens. Thus, Bobin et al.[88], focusing a pulse of 2 GW power with a lens of f = 5 cm obtained a plasma-boundary propagation velocity 8×10^7 cm/sec. When long-focus lenses are used, the breakdown occurs at discrete points on the laser-beam axis. Thus, Basov et al.[89], who used pulses of ≈ 1 GW power and a lens of focal length 2.5 m, obtained a laser spark, which they called "long," consisting of a set of individual sparks with a total length exceeding 2 m. The breakdown occurred at the focus and then propagated towards the lens with a velocity 2.2×10^9 cm/sec, and in the opposite direction with a velocity 3.8×10^9 cm/sec. The character of the breakdown development is attributed by the authors to the time variation of the spatial structure of the laser radiation.

At powers on the order of hundreds of MW, the detonation-wave and breakdown-wave propagation velocities are close to each other, and small changes in the experimental conditions can lead to a transition from one regime to another. Thus, Daiber and Thompson[71] interpreted their results from the point of view of the detonation mechanism, while Alcock et al.[77,78] explained their results, obtained practically under the same conditions, from the point of view of the breakdown mechanism. The intermediate cases, when a small change of the laser pulse parameters led to a transition from one regime to another or when the propagation of the plasma proceeded via successive breakdowns with a hydrodynamic regime between them, were observed by Korobkin et al.[90] and by Daiber and Thompson[91].

f) Temperature measurement. The single-valued relation between the internal energy of the gas and the detonation-wave velocity (see formula (15)) makes it possible, under the conditions of the hydrodynamic regime, to estimate the gas temperature from the measured values of the velocity of the plasma boundary towards the lens. For example, Mandel'shtam et al.[83] obtained by this method a temperature 7×10^5 °K.

In a number of studies[83,91-93], the plasma electron temperature was determined from the spectrum of the recombination radiation in the soft x-ray region. The values of T_e measured in[91,92] range from 0.4×10^6 to 1.8×10^6 deg. In[92] it was shown that the duration of the x-radiation does not exceed the duration of the laser pulse. Measurements performed with spatial resolution[91] have shown that the x-radiation is emitted only from the brightly glowing region adjacent to the front of the absorption wave.

Still higher temperatures, $T_e \approx 300$ eV (3×10^6 deg), were measured by Vanyukov et al.[93] In these experiments, a laser spark was produced in air and in a mixture of air with deuterium by focusing a 6-GW pulse of 20 nsec duration.

Korobkin et al.[90] estimated the ion temperature of the plasma from the lateral-expansion velocity. The obtained value $T_i \approx 6 \times 10^5$ °K agrees sufficiently well with the electron temperature determined by measuring the radiation in the soft x-ray region[83]. Komissarova et al.[85] estimated the plasma temperature at instants corresponding to the end of the laser pulse from the velocity of the lateral expansion. Considerable longitudinal temperature gradients were observed.

g) Measurements of electron concentration. Interference, holographic, and spectroscopic methods were used to measure the electron concentration in a laser-spark plasma. Most measurements performed by the interference and holographic methods, and practically all the spectroscopic measurements, pertain to the later stages of the laser-spark development (after the termination of the laser pulse), but a number of studies covered also stages corresponding to the action of the laser radiation on the plasma. Thus, Alcock et al.[94] measured by an interference method the electron concentration in a laser spark in air at an instant of time approximately 30 nsec after breakdown ($n_e \approx (3-5) \times 10^{19}$ cm^{-3}). Values of the same order, $n_e \approx (2-3) \times 10^{19}$ were obtained by a holographic method in[95-97] for the stage corresponding to 40 nsec after the production of the spark.

Komissarova et al.[85] investigated, by the method of two-long-wave holographic interferometry, the spatial distribution of the electron density in a laser spark in air for instants from 30 to 110 nsec after breakdown (see Fig. 10a). Considerable gradients of the electron concentration were observed at instants of time when the plasma was still acted upon by the laser radiation (30—65 nsec). It is shown in that paper that the loss of electron concentration during the investigated stage is due mainly to the expansion of the region occupied by the plasma. The number of electrons integrated over the volume remains practically unchanged in the time from 30 to 65 nsec. A similar procedure was used to determine the electron concentration in a laser spark in hydrogen and in helium[86]. In all cases when the initial gas pressure exceeded 6 atm, considerable gradients of the electron concentration was observed, analogous to those observed in the laser-spark plasma in air[85]. At low pressures, the gradients of n_e were observed only for the earliest instant of time (20 and 30 nsec), or were even completely absent (for example, for a spark in hydrogen at a pressure 1.75 atm; see Fig. 10b).

Interference measurements of the electron concentration in a laser spark in xenon were carried out by Hugenschmidt[98-100].

It should be noted that the electron concentrations registered in all the investigations are lower by approximately one order of magnitude than the values expected in the case of an equilibrium (thermal) ionization of the gas at the initial density. To be sure, it is impossible as a rule to register the shifts of the interference fringes in the zone directly adjacent to the absorption-wave front. In those sections where the electron concentration

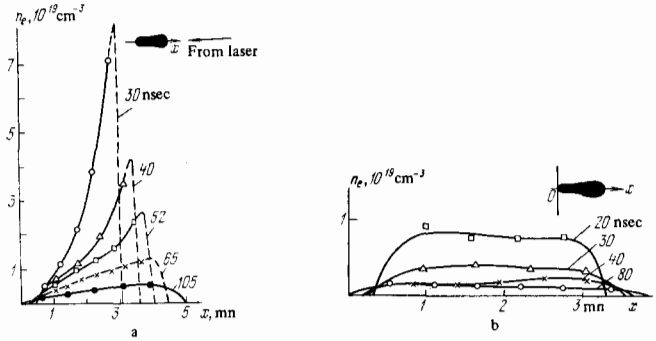

FIG. 10. Distribution of electron concentration along the longitudinal axis of a laser spark. a) Spark in air, p = 1 atm [85]; b) spark in hydrogen, p = 1.75 atm [86].

can be measured, the mass density of the gas is much lower than the initial density even during the early stages of the existence of the laser spark.

It follows from an examination of the experimental data that the laser-spark plasma parameter change significantly during the time of action of the laser radiation. The high temperatures determined by measuring the x-radiation pertain to a very narrow rapidly moving layer directly adjacent to the absorption wave. It is here that the maximum electron concentrations are likewise observed. This layer screens the plasma regions behind it, which, since they do not receive additional energy, expand and cool down. This results in the appreciable electron-concentration and temperature gradients observed in[85,86]. If the laser spark is produced in light gases at relatively low pressures, the energy-release zone is not localized in a region adjacent to the plasma boundary. Then no predominant motion of the plasma boundary in a direction opposite to the laser radiation is observed[71], nor are there any gradients of the electron concentration and of the temperature[86].

h) Features of the development of a laser spark produced by pulses of picosecond duration. The development of a laser spark produced by a single pulse of duration 10^{-11} sec was investigated by Alcock et al.[63]. The plasma-radiation scans obtained with an image converter show a bright center of ≈0.1 mm diameter, which exists for several dozen nanoseconds, and a less bright envelope, expanding with an initial velocity $\approx 4 \times 10^8$ cm/sec. The authors of[63] believe that this glow may be caused by ionization of the surrounding gas layers by the short-wave radiation emitted from the hot center.

If the laser spark is produced by a train of picosecond pulses, then, as already noted, the breakdown produced by individual pulses of the train occurs at discrete points regularly distributed along the beam axis. These points are seen on spark photographs obtained in the light of the laser radiation[60]. The scans of the plasma glow itself[62,101] also show that the arrival of each succeeding pulse causes a jumplike propagation of the plasma towards the laser. The initial propagation velocity of the glowing region, according to[101], is approximately 3×10^8 cm/sec and corresponds apparently to photoionization of the gas by the radiation of the hot plasma. In the period between the individual pulses, the average velocity is $\approx 7 \times 10^6$ cm/sec, and corresponds to free expansion of the plasma.

An attempt to explain the jumplike development of the breakdown and the corresponding periodic structure of the scattered radiation was made by Wang and Davis[60]. The breakdown produced by the first picosecond pulse is regarded as the center of a spherical explosion wave. The arrival of the next pulse produces breakdown on the shock front of this wave, and the breakdown point itself becomes the center of a new spherical shock wave, etc.

Information on the parameters of a plasma produced in the breakdown of gases by picosecond pulses is practically nonexistent. Data on the plasma temperature are given only by Gorbeko et al.[101], who estimated the ion temperature corresponding to ≈2 nsec after the breakdown at $T_i \approx 6 \times 10^6$ °K, as determined from the initial free-expansion velocity of the plasma (4×10^7 cm/sec).

i) Laser spark produced by focused CO_2 radiation. The development of the laser spark produced by radiation from pulsed CO_2 lasers was investigated in[102-104]. Gravel et al.[102] and Tomlinson[103] used for the production of the laser spark a pulse with a total duration up to several microseconds, and the bulk of the energy was contained in its leading section of 300—400 nsec duration. During this part of the pulse, the plasma propagated towards a focusing mirror at a velocity governed to the detonation mechanism. The motion was then abruptly slowed down. The calculations show that the mean free path of the laser-emission quanta was, up to this instant of time, of the order of the radius of the light channel, corresponding to the limiting conditions for the existence of a detonation wave. The abrupt slowing down of the motion corresponded to a transition from the detonation regime to the so-called "slow burning" regime (see below). Motion of the plasma boundary in two directions towards the lens and away from it, with approximately constant velocity, was then observed, thus indicating relatively small absorption of the radiation in the plasma. Gravel et al.[102] have observed at 1.5 μsec following the breakdown, in a region close to the focus, a glowing filament propagating with a constant velocity $\approx 10^6$ cm/sec in the direction of the laser radiation. They explain the observed picture in the following manner: When the plasma becomes almost completely transparent, a second breakdown occurs near the focus on the boundary between the plasma and the neutral gas. The shock wave again propagates in two directions, but the front moving through the already-expanding plasma absorbs practically no laser radiation. The energy release occurs on the front propagating in the opposite direction. This, of course, explains neither the constant propagation velocity nor the filamentary structure of the plasma formation. The presence of a plasma in the focal region seems to influence in some way the character of the radiation propagation behind the focus.

Breakdown induced by a train of pulses from a mode-locked CO_2 laser (duration of each pulse ≈3 nsec, intervals between them ≈25 nsec, total duration of train ≈400 nsec) was observed in[104]. The picture was very similar to the breakdown of gas by a train of picosecond pulses from a neodymium laser[60].

j) Laser spark in the regime of "slow combustion" and constantly burning optical discharge. As already noted[72], much less radiation intensity is required to maintain the detonation regime than to produce the laser spark. However, another mechanism of plasma propagation is possible, at even lower radiation intensities. This regime was called "slow burning." In this case, new layers of gas become capable of absorbing the radiation as a result of their heating by heat conduction.

The first to observe a laser spark in the slow-burning

regime were Bunkin et al.[105]. The spark was ignited by an extraneous source (by a spark discharge between electrodes). The radiation from a neodymium laser operating in the free-generation regime (E = 1000 J, Δt = 2.5 msec) was focused with a long-focus lens in such a way that the diameter of the focal spot was 3 mm. Under these conditions, the radiation intensity was ≈ 10 MW/cm^2, which is approximately one order of magnitude less than required to maintain the detonation regime, and two orders of magnitude less than the threshold intensities needed for spontaneous breakdown. Under the influence of the radiation, the plasma boundary propagated in both directions away from the focus of the lens with an approximate velocity 50 m/sec.

Detailed calculations of the radiation intensity needed to maintain the "slow burning" regime, and also of the rates of propagation of the plasma boundaries and its temperature, are given in the papers by Raĭzer[106-108].

The "slow burning" regime was obtained also by Mul'chenko et al.[109]. A laser spark in argon at a pressure of 80 atm was ignited by a beam from a ruby laser operating in the spike regime, and the "slow burning" was maintained by using a ruby laser in the quasicontinuous regime, generating a smooth pulse of 1.5 msec duration and 50 J energy. After several dozen microseconds following the application of the maintaining pulse, the leading front of the plasma was detached from the point of ignition and propagated in a direction opposite to the laser radiation, with an initial velocity 250 m/sec.

Raĭzer[106-108] calculated the radiation power needed to maintain a continuously burning optical discharge ("optical plasmotron"). This discharge was first produced by Generalov et al.[110] using a cw CO_2 laser. The discharge was ignited by a pulsed CO_2 laser, the radiation of which was focused at a right angle to the radiation of the cw laser that maintained the discharge. To maintain a discharge in xenon at 2—4 atm, 150 W of power was sufficient. The plasma was symmetrical relative to the focus of the lens, thus evidencing incomplete absorption of the radiation. The plasma temperature was estimated at $\approx 15\,000$°K. More detailed information on the results of the experimental investigation of a constantly glowing optical discharge can be found in[111].

k) Laser radiation scattered by a laser spark. Spark-scattered laser radiation was investigated by a number of workers. As already noted, the scattering-line shift relative to the laser-emission line was interpreted as a Doppler shift due to the motion of the detonation wave towards the focusing lens[68,83,90].

It is known that scattering of laser radiation by electrons is widely used for plasma diagnostics. In the first investigations of laser sparks[68,83] attempts were therefore made to determine the plasma parameters from the laser emission scattered by the spark. The electron temperature estimated from the width of the scattered-radiation line turned out to be much lower than that measured by other methods. It was subsequently shown that the intensity of the scattered radiation exceeds by several orders of magnitude the value calculated under the assumption of Thomson scattering[36,112-114], and it was concluded that the scattered radiation is due to reflection and refraction of the laser radiation by the shock-wave front and in the highly-ionized region near the focus of the lens, and cannot be used for plasma diagnostics.

Photographs of the laser spark in the light of the scattered radiation reveal a bead-like structure[83,90]. The time scans of the spark show that the scattering centers occur in succession, and move towards the lens. These centers were interpreted as discrete regions of breakdown. However, Savchenko and Stepanov[115] have observed that on photographs taken simultaneously from points located on opposite sides of the spark the bead-like structures differ greatly in the number of scattered centers, and have reached the conclusion that the scattering is not a volume but a surface effect connected with reflection and refraction of the radiation by the plasma boundary. Analogous conclusions were drawn also in[113], where it was shown that the small dimensions of the scattering centers can be explained from geometrical considerations, by considering the reflection of the laser beam from the spherical surface of the wave front. Thus, the smallness of the apparent dimensions of the scattering centers cannot serve as proof of presence of such small plasma formations.

Korobkin and Alcock[116] have observed that when a laser spark is produced with a single-mode ruby laser, the scattering region takes the form of filaments of diameter not larger than 5 μ. The appearance of these filaments is attributed by the authors to self-focusing of the laser radiation.

A similar filamentary structure was observed in[59,114]. It was noted that in molecular gases the scattering region takes the form of almost solid filaments. After they are produced, the filaments move towards the laser at a gradually decreasing velocity (the initial velocity, according to the data of[59] is 1.5×10^7 cm/sec). In inert gases, the filaments have a lifetime of only a few nanoseconds, after which their propagation slows down abruptly and a new filament is produced several microns ahead of the preceding one, as a result of which the scattering region takes the form of discrete centers. It was shown in[117] that the number of scattering centers and the distances between them depend on the pressure of the gas in which the spark is produced.

In the case of gas breakdown by a series of picosecond pulses[60,118], the structure of the scattering region takes the form of individual points measuring not more than 10 μ and disposed along the axis of the laser.

Bunkin et al.[65] observed, intense scattering centers not accompanied by breakdown were produced by focused picosecond pulses at a power somewhat lower than the threshold value in air and nitrogen. Following a slight increase in the power, breakdown occurred in one or several of these points, accompanied by a repeated flash of scattered radiation. The results were attributed to the self-focusing mechanism.

The angular distribution of radiation scattered by a spark was investigated in[59,60,116,118,119]. In the plane perpendicular to the laser axis, the intensity of the scattered radiation varied approximately like $\cos^2\theta$ ($\theta = 90°$ corresponds to the electric-field intensity vector having the same direction as the laser radiation)[119]. An intense peak of scattered radiation is observed in the forward direction in the plane containing the laser beam. When the laser spark is produced with the aid of a

single-mode laser[59,116], an appreciable fraction of the laser-pulse energy was scattered in the forward direction (within a cone of angle 30°). For argon, the fraction of the scattered radiation reached 80% of the incident radiation. Similar results were obtained also when the spark was produced with picosecond pulses[60,118].

The spectral characteristics of the forward-scattered radiation were investigated in[59,120]. Line broadening accompanied by a shift towards longer wavelengths was observed in molecular gases, whereas an anti-Stokes shift of the broadened line was observed in inert gases. When the spark was produced with the aid of picosecond pulses, the broadening reached 200 Å. The spectral characteristics of the scattered radiation are quite similar to those observed in the self-focusing of laser radiation in liquids.

l) Self-focusing. The smallness of the scattering regions, and the angular and spectral distributions of the scattered radiation can be ascribed to self-focusing of laser radiation accompanying breakdown in gas. All these effects offer, however, only indirect evidence of self-focusing, since neither the structure of the laser beam near the focus nor the plasma produced by it has been observed directly. Direct evidence of self-focusing are the recently observed[121-123] plasma filaments preceding the formation of the principal breakdown regions.

Self-focusing can be observed in substances whose refractive index is increased by the radiation. In gas breakdown, self-focusing can occur in a neutral gas prior to breakdown, during the breakdown when a partially ionized gas with a large number of atoms in different excitation states is present, and finally in the plasma.

The first of these possibilities is not very likely for two reasons[59,114]. First of all, if the self-focusing were to occur in a neutral gas, then the breakdown threshold would correspond to the self-focusing threshold and not to the ionization threshold. However, the agreement of both the absolute values of the threshold intensities and of the observed dependence of the breakdown threshold on the experimental conditions with the predictions of the theory of cascade ionization makes such an assumption unlikely. In addition, such possible self-focusing mechanisms as electrostriction, the Kerr effect, and nonlinear electron polarizability lead in the case of gases to threshold powers that greatly exceed those at which self-focusing is observed in gas breakdown. Thermal effects, at particular intensity distributions in the beam, can lead to self-focusing (see, e.g., [124,125]). As a rule, however, gas heating by radiation absorption leads to a decrease in the density and in the refractive index on the beam axis and to defocusing. In addition, the thermal effects are subject to inertia and cannot be responsible for self-focusing of *nanosecond* and picosecond pulses. The second possibility is the onset of self-focusing in the plasma during the breakdown or after the breakdown. In the initial stage of the breakdown process the focal region contains a mixture of electrons, ions, and excited atoms. As is well known, the presence of the electrons decreases the refractive index, and if the electron concentration is maximal on the laser-beam axis, this should lead not to self-focusing but to defocusing of the radiation. An increase of the refractive index within the confines of the laser beam can be expected as a result of the appearance of excited atoms.

A mechanism of self-focusing of the radiation following excitation of atoms and molecules was proposed by Askar'yan[126]. The polarizability of the excited atoms can greatly exceed the polarizability of the atoms in the ground state. At sufficiently large concentration of the excited atoms, the increase of the refractive index as a result of their polarizability may not only cancel out the action of the electrons, but lead also to an increase of the refractive index on the beam axis and to self-focusing. As shown in[121], the cubic nonlinear polarizability of the excited atoms can be 10^9 times larger than the corresponding value for unexcited atoms. The threshold power of the self-focusing in argon as a result of the excited atoms is estimated in that paper at $\approx 10^4$ W.

The self-focusing of electromagnetic radiation in a plasma has been the subject of a number of papers (see, e.g.[127-130]). Strong electromagnetic radiation applied to a plasma causes a redistribution of the electrons and ions. The electrons are crowded out from the region where the electromagnetic field is maximal. This electron motion continues until the forces exerted on the plasma by the electromagnetic field are balanced by the gas-dynamic pressure. This leads to a decrease of the electron concentration and to corresponding increase of the refractive index on the laser-beam axis, which in turn can lead to self-focusing.

The threshold self-focusing powers in gas breakdown were estimated in[129,130]. They are close to the values at which plasma filaments have been observed in experiments.

Thus, calculations show that from among the considered mechanisms at least two, nonlinear polarizability of the excited atoms and the change of the spatial distribution of the electrons in the electromagnetic-radiation field, have threshold powers close to those at which self-focusing is observed in breakdown in gases.

Self-focusing filaments were first observed directly in[121], for argon breakdown by a laser pulse of ≈ 2 MW power. A Schlieren photography technique with a time resolution 0.5 nsec was used for the observation. Filaments of diameter less than 10 μ were observed. A more complicated structure connected with the breakup of the filament and the formation of plasmoids was observed on the end of the filament farther from the laser.

A detailed interferometric investigation of plasma filaments produced in the breakdown of a large number of gases was carried out by Richardson and Alcock[122]. They have observed that the filaments propagate from the focus towards the laser with a velocity $\approx 4 \times 10^7$ cm/sec. A plasmoid is produced on the end of the filament farther from the laser. In inert gases, new plasmoids are produced along the propagating filament, spaced 200—300 μ apart, and the filaments gradually vanish between the plasmoids. In molecular gases, the main plasma region propagates continuously along the filament towards the focusing lens. After the formation of the main plasma region, a narrow center, in which the electron concentration is approximately one order of magnitude larger than the average electron concentration in the plasmoid, can be traced for 1—2 nsec after the formation of the main plasma region. Figure 11 shows the interference pattern of the plasma filament (a) and the distribution of the electron concentration as well as the variation of the diameter along the filament (b). The decrease in the refractive index, observed as a result of the interference investigation of the filaments, should in itself lead not to self-focusing but to defocusing of the radiation. It appears that the self-focusing precedes the

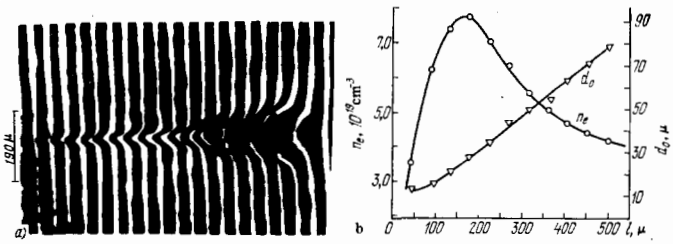

a FIG. 11. Interference pattern of plasma filament (a) and distribution of the electronic concentration n_e and the variation of the diameter d_0 along the filament (b) [122].

formation of the high-ionized plasma within the confines of the filaments.

Self-focusing filaments were observed also by Belland et al.[123] in breakdown in air. The ruby-pulse duration was in this case 1.6 nsec and the power was 1.5 GW. At the instant of time corresponding to the onset of the breakdown, a filament of diameter not larger than 15 μ was observed. This was followed by two more filaments. This breakup of the optical channel into a number of filaments is typical of the case when the power greatly exceeds the self-focusing threshold.

Thus, experimental investigations[121-123] have yielded undisputed proof of self-focusing occurring during gas breakdown by laser radiation. However, neither the self-focusing mechanism nor the dynamics of its development have been made clear so far. The plasma filaments observed in these papers are not the cause but the consequence of the self-focusing. It can only be stated that the self-focusing precedes the formation of the principal plasma region and occurs apparently during the course of the breakdown development.

Self-focusing was observed in the breakdown of different gases by pulses of durations from several picoseconds to 30 nsec, and at powers from 2 MW to several GW, with both single-mode and multimode lasers. The onset of self-focusing should influence strongly the course of the various processes connected with breakdown development, since the cross section of the optical channel, and consequently also the radiation density, should differ significantly in this case from those calculated without allowance for self-focusing. In particular, the appreciable discrepancy between calculations that do not take self-focusing into account in experiment is evidenced by the results of[65,123], where a distinct dependence of the breakdown threshold on the dimensions of the focal volume was observed under conditions when the diffusion losses are small[123] or practically nonexistent[65] (breakdown produced by picosecond pulses). The authors of the last reference attribute their results to self-focusing in the neutral gas, as a result of which the diameter of the optical channel decreases to a value d_c which depends little on the initial dimensions of the focal region. At the powers employed in that reference (on the order of several GW), the self-focusing mechanism can be the nonlinear electron polarizability. Further contraction of the channel to a value ≈ 10 μ occurs, in the authors' opinion, during the course of the breakdown as a result of the appearance of excited atoms and molecules.

4. LATER STAGES OF LASER-SPARK DEVELOPMENT

a) Shock wave propagation. After the termination of the laser pulse, there remains a region of sufficiently dense ($n_e \approx 10^{19}$ cm^{-3}) and hot plasma ($T \approx 10^5$ deg). The plasma expansion, which started already during the time of absorption of the laser-radiation energy, continues. A shock wave is produced and is clearly seen on the laser-spark interference pattern starting with instants of time 60—100 nsec after the occurrence of the breakdown[86,94].

The shock wave propagation can be described in first-order approximation by the theory of a strong detonation from a point[131,132]. The law governing the motion of the shock wave in the case of spherical symmetry is given by

$$r=\xi_0\left(\frac{E}{\rho_0}\right)^{1/5}t^{2/5}, \tag{21}$$

where E is the energy released at the center of the detonation, ρ_0 is the initial gas density, and ξ_0 is a dimensionless constant that depends on the effective adiabatic exponent γ. The shock-wave propagation velocity is equal to

$$D=\frac{dr}{dt}=\frac{2}{5}\xi_0\left(\frac{E}{\rho_0}\right)^{1/5}t^{-3/5}. \tag{22}$$

However, the real case of the propagation of a shock wave initiated by a laser spark differs significantly from the idealized problem of detonation from a point. First, the energy release occurs not instantaneously, but after a time comparable with the laser-pulse duration, and not from a point, but from a volume of finite size (10^{-4}—10^{-5} cm^3). This is usually a cone with an apex angle $\approx 10°$ and a height of several millimeters. As a result, the laser spark has from the very beginning not a spherical but a pear shape. In the course of time, the shape of the front approaches that of a spherical one, but by that time the pressure on the shock-wave front becomes comparable with the pressure of the surrounding gas, and the propagation of the shock wave should be described by explosion theory with the back pressure taken into account[132]. In addition, owing to the finite dimensions of the volume from which the energy is released, the temperature at the center of the laser spark is finite, and the gas density differs from zero, whereas according to the theory of detonation from a point the temperature tends to infinity and the density to zero as the center is approached.

An attempt to calculate the shape and motion of the shock-wave front for the case when the energy is released from a conical volume was made by Panarella and Sovic[133]. The problem was solved by the perturbation method assuming self-similarity. The calculated shape of the shock wave agrees well with that observed in[94]. It follows from the theoretical analysis that the difference between the axes of the oval by which the shock wave can be approximated should vary very slowly with time.

The experimental study of shock-wave propagation is the subject of many works[84,85,86,134-136]. Alcock et al.[94] obtained good agreement between the density profiles behind the shock-wave front, calculated from the interference patterns, and those predicted by the strong-explosion theory.

The time variation of the longitudinal and transverse dimensions of the laser spark were investigated in[94,85,86,134]. Figure 12 shows the time variation of the dimensions of a laser spark in air, determined from shadow photographs[134]. As seen from the figure, the difference between the longitudinal and transverse

dimensions remains practically constant in time, in agreement with the theoretical calculations[133].

A detailed comparison of the propagation of the shock wave from a laser spark with the theory of detonation from a point is given in[135,136]. Figure 13 shows the ratio of the shock-wave energy E_{sw} to the total laser-pulse energy E, obtained in[135], as a function of the gas pressure. We see that for He and H_2 the fraction of the energy contained in the shock wave increases with increasing pressure, this being due to the increase of the plasma absorption coefficient. The curves for N_2, Ar, and Xe exhibit maxima, the appearance of which, in the authors' opinion, is due to the increased energy loss to radiation during the time elapsed from the production of the plasma to the detachment of the shock wave from it.

b) Detachment of the shock-wave front from the luminous region. A strong explosion is characterized by the detachment of the shock wave from the luminous region, called the "fireball."[137,138]. The detachment occurs at the instant when the shock wave velocity, and consequently the temperature behind the shock-wave front, decrease to values insufficient for a noticeable ionization in excitation of the gas. This phenomenon is observed also in the propagation of a shock wave initiated by a laser spark (Fig. 14[139]). As seen from the figure, the detachment of the region of the H_α line emission (the laser spark was obtained in a mixture of air with hydrogen) from the shockwave front occurs at a time ≈ 200 nsec and at a shock-wave velocity ≈ 10 km/sec, corresponding to a temperature $\approx 15{,}000^\circ$ behind the shock-wave front in air (see[137]).

It is of interest to compare the radius r_{fb} of the fireball at the instant when the shock wave is detached from it and the detachment time t_{fb} for a laser spark and for a powerful nuclear explosion. If it is assumed that the detachment occurs at a certain shock-wave critical velocity D_{cr}, then we obtain for the instant of detachment, in accordance with (22),

$$t_{fb} = \left(\frac{2}{5}\xi_0\right)^{5/3} D_{cr}^{-5/3} \left(\frac{E}{\rho_0}\right)^{1/3}. \quad (23)$$

The fireball radius at the instant of detachment is obtained by substituting t_{fb} in (21):

$$r_{fb} = \left(\frac{2}{5}\right)^{2/3} \xi_0^{5/3} D_{cr}^{-2/3} \left(\frac{E}{\rho_0}\right)^{1/3}. \quad (24)$$

Thus, when the explosion energy is varied, the instant of detachment and the radius of the fireball should vary like $E^{1/3}$. For a nuclear explosion in which the energy released is $E_{ne} \approx 10^{21}$ erg, the detachment of the shock wave occurs approximately 15 msec after the explosion, and the radius of the fireball at that instant is ≈ 100 m[138]. For a laser spark produced by a laser pulse with energy $E_{ls} \approx 0.5$ J $= 5 \times 10^6$ erg, the corresponding values should be smaller by a factor $(E_{ne}/E_{ls})^{1/3} \approx 6 \times 10^4$. Thus, in the case of the laser spark we obtain for the instant of detachment of the shock wave $t_{fb} = (1.5 \times 10^{-2})/(6 \times 10^4)$ sec $= 250$ nsec, and the radius of the fireball is in this case $r_{fb} = 10^4$ cm$/(6 \times 10^4) = 1.7$ mm, which agrees quite well with the measured values $t_{fb} = 200$ nsec and $r_{fb} = 1.2$ mm (see Fig. 14).

The analogy between a nuclear explosion and the laser spark was pointed out by Askar'yan et al.[140]. In that paper, the volume of the highly-ionized region V_{fb} was estimated from the perturbation of the external magnetic field. Their measured value $V_{fb} = 10^{-4}$ cm^3 is however, considerably lower (by two orders of magnitude) than the volume of the laser spark at the instant of detachment of the shock wave, as given in[139].

c) Ionization aureole. In the case of powerful explosions, the aureole stage preceding the shock-wave formation is characterized by a radiative expansion of the fireball[137,138]. The x-rays emitted by the hot region are absorbed in the surrounding layers of air and heat it to high temperatures. This type of radiation expansion of the luminous region was observed also in gas breakdown by picosecond pulses[63,101]. The initial expansion velocity of the luminous region was $(3-4) \times 10^8$ cm/sec.

In the breakdown of a gas by nanosecond pulses, the gas layers surrounding the plasma do not have time to become heated to high temperatures during the time of the development of the hydrodynamic motion. Nonetheless, the absorption of soft x-rays and short-wave ultraviolet radiation leads to ionization of the gas layers adjacent to the plasma. This phenomenon was discussed by Askar'yan et al.[141] and called the "ionization aureole." It is also the subject of[142,143]. The overlap of the ionization aureole with the microwave radiation was used to estimate the dimensions of the aureole ($r \approx 1-2$ cm) and the lower limit of the electron concentration in it ($n_e \approx 10^{13}$ cm^{-3}). The ionization-aureole lifetime depends on the type of gas. Separation of the ionization flash of the fast aureole, due to the absorption of the radiation, from the slow glowing ionization accompanying the propagation of the shock wave, was observed in a number of gases. This "slow" aureole lasts quite a while ($\approx 10^{-4}$ sec).

Thus, several nanoseconds after the end of the laser pulse, the laser spark constitutes a formation with a rather complicated structure: a hot center is surrounded by layers of colder gas heated by the shock wave, and the shock-wave front is in turn surrounded by a cloud of

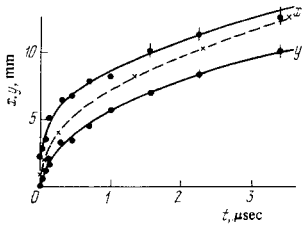

FIG. 12. Time variation of longitudinal (x) and transverse (y) dimensions of the spark [134]. Dashed line—theoretical curve for a spherical shock wave.

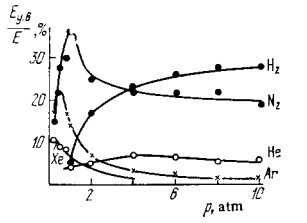

FIG. 13. Ratio of the shock-wave energy to the total laser-pulse energy as a function of the gas pressure [135].

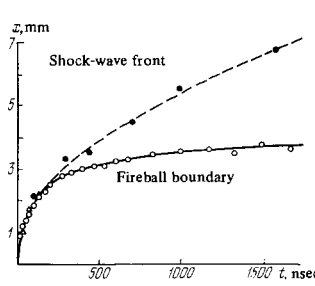

FIG. 14. Detachment of shock-wave front from the region of the H_α-line emission [139].

weakly-ionized plasma produced by photoionization. Most experimental determinations of the laser-spark plasma parameters during the later stages of the spark development pertain to the hottest central region of the plasma.

d) Measurement of the electron concentration. The electron concentration in a laser-spark plasma after the end of the laser pulse was determined by the methods of usual and holographic interferometry, and also by spectroscopic methods—from the Stark contours of the spectral lines.

In interferometry measurements it is necessary to take into account the fact that the shifts of the interference fringes of the laser spark are due both to the presence of the electron gas and to the decrease of the concentration of the heavy particles in the central regions of the plasma. To measure the electron concentration it is therefore necessary either to obtain interference patterns at two wavelengths, or to make certain assumptions concerning the redistribution of the atom concentration in the laser spark.

Measurement of the electron concentration in the laser spark by the method of two-wavelength interferometry was carried out by Alcock and Ramsden[144].

Komissarova et al.[145] investigated by the method of holographic interferometry the radial distribution of the electron density in a laser-spark plasma in air during the first 200 nsec after the breakdown (Fig. 15). What is typical is the absence of some considerable electron-concentration gradients near the center of the laser spark. At ≈ 100 nsec after the start of the breakdown the longitudinal gradients of the electron density, which exist during the earlier stages, also become equalized (see Fig. 10). It appears that this is also evidence of the relative constancy of the temperature and of the concentration of the heavy particles in the inner regions of the spark during these stages. It was shown in[145] that the total number (integrated over the volume) of the electrons in the plasma ($\approx 3 \times 10^6$) remains practically constant in the time interval from 84 to 210 nsec.

An interference-holographic investigation of the laser spark in air, in the interval from 1 to 38 μsec, is reported also in[146]. Hugenschmidt[90-100] investigated a laser spark in xenon by interferometry. The electron-concentration profiles observed in these studies, as in the case of a laser spark in air (Fig. 15[145]), are flat near the center of the plasma and terminate abruptly at a distance ≈ 0.7 of the shock-wave front radius.

In a number of studies, the electron concentration in the laser spark was determined from the Stark contours of the spectral lines emitted by the plasma. Time scans of the spectral-line contours for a spark in a mixture of hydrogen and helium were obtained by Evtushenko et al.[147] The widths of the lines H_α and He I λ 5876 Å changed during the first microsecond from 200 to 20 Å, corresponding to a change in the electron concentration from 10^{19} to 5×10^{17} cm^{-3}.

The electron concentration in the plasma of a laser spark in hydrogen was determined from the spectral-line contours by Litvak and Edwards[148]. The time variation of the electron density in a laser spark in helium was investigated by an analogous method in[149,150]. Spectroscopic methods were used in[149] to investigate the spatial structure of the laser-spark plasma in helium.

Evtushenko et al.[151] determined the concentration of the electrons in a spark in hydrogen from the contours of the H_α line in absorption.

A microwave procedure was used in[152] to determine the electron concentration in a laser spark. The laser spark was obtained at the center of a resonator of the Fabry-Perot type. The measurements covered the time interval up to 10^{-3} sec after the breakdown, when the electron concentration is so low ($\approx 10^{14}$ cm^{-3}) that its measurement by optical methods is no longer possible.

The time variation of the electron concentration in a laser spark in the interval from 100 nsec to several microseconds, as obtained by various workers, is shown in Fig. 16.

The change of the electron concentration is due to two factors: hydrodynamic expansion and recombination processes. For a laser spark in hydrogen during the initial stage of expansion, the degree of ionization is close to unity and $n_e \sim \rho$. The character of the time variation of the gas density ρ in the central region of the laser spark, owing to the finite volume from which the energy is released, should differ significantly from that given by the theory of detonation from a point. At this same time, the time variation of the shock-wave dimensions, in accordance with the experimental data, can be described in first order by formula (21), which follows from the theory of detonation from a point according to which $r \sim t^{2/5}$. If it is assumed that the gas density at the center is inversely proportional to the volume occupied by the shock wave, then we have for spherical geometry $n_e \sim r^{-3} \sim t^{-6/5}$. This corresponds to a slope -1.2 for the plot of the function $\log n_e = f(\log t)$, which is close to that observed in most studies. For the later instants of time, when the counter pressure must be taken into account, the character of the volume expansion changes. On the other hand, as the plasma becomes cooler, the role of recombination processes in the change of n_e increases. Recombination in a laser-spark plasma in hydrogen and helium is dealt with in[148,149].

e) Measurement of plasma temperature. The first

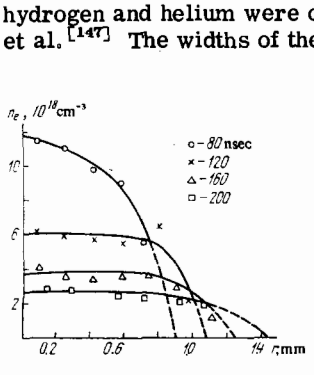

FIG. 15. Radial distribution of electron concentration in a laser-spark plasma in air (p = 1 atm). [145].

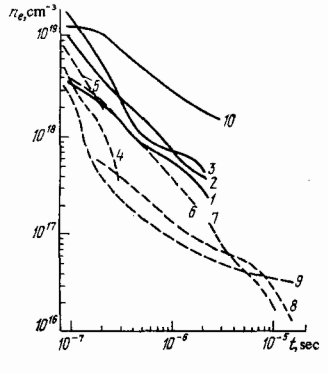

FIG. 16. Time variation of the electron concentration in a laser spark. 1–H_2, 4 atm [148]; 2–H_2, 8 atm [148]; 3–H_2, 6 atm [151]; 4–air, 1 atm [144]; 5–air, 1 atm [145]; 6–He, 4 atm [150]; 7–He, 5 atm [149]; 8–He, 0.75 atm [153]; 9–He, 0.5 atm [193]; 10–Xe, 1.4 atm [98-100].

estimates of the electron temperature in a laser-spark plasma in air were made by Mandel'shtam et al.[154]. The temperature was determined from the ratio of the intensities of the N_{II} line in the time-integrated spectrum of the laser spark. The obtained value $T_e \approx 5 \times 10^4$ °K pertains to the later stage of the spark development (after the end of the laser pulse).

The change of temperature with time was investigated for a laser spark in hydrogen by Litvak and Edwards[148]. The temperature was determined from the ratio of the intensity of the H_α line to the intensity of the continuous spectrum. A similar procedure was used to determine the temperature of a laser spark in helium in[150].

In a number of studies, the temperature was determined from the ratio of the emissivity of the plasma and its absorbtivity[151,155]. Hugenschmidt[100] determined the temperature of a laser-spark plasma in xenon from the spectral distribution of the continuous radiation in the ultraviolet region.

Figure 17, constructed from data by various authors, gives plots of the temperature against the time. In most cases the temperature decreases quite rapidly during the first several hundred nanoseconds after breakdown, and then remains practically constant. A very weak dependence of the temperature on the time was observed for a laser spark in helium in[153,155]. The decrease of the temperature in the initial stage of expansion is the result of adiabatic expansion of the plasma. Subsequently, the change of temperature slows down, and this may be due, on the one hand, to slowing down of the expansion and, on the other, to the release of additional energy upon recombination. In particular, the very slow time variation of the laser-spark plasma temperature in helium appears to be due to recombination processes[149,150].

f) Measurement of the concentration of heavy particles in a plasma. As already noted, the character of the variation of the heavy-concentration particle and its spatial distribution should differ significantly from those given by the theory of detonation from a point. Therefore measurement of the gas density in the central region of the laser spark is of special interest.

Methods of two-long-wavelength interferometry make it possible, in principle, to measure the concentration of heavy particles in a plasma. Komissarova et al.[85,86] have shown that 60 nsec after the breakdown the heavy particles are already practically completely pushed out into the shock wave. However, the accuracy of the interferometer measurements allows us only to state that the concentration of the heavy particles in the central regions is smaller than a certain limiting value n_{lim} ($n_{lim} \approx 5 \times 10^{18}$ cm^{-3} for air). The estimate $n_a < 10^{17}$ cm^{-3}, given by Hugenschmidt et al.[99] for the concentration of the atoms in the central zone and obtained by reducing two-long-wavelength interference patterns of the spark in xenon, seems to us to be significantly underestimated, inasmuch as in that study they determined in fact the concentration of not the atoms alone, but of all the heavy particles, including the ions, so that it is difficult to reconcile the result with the electron density $n_e \approx 3 \times 10^{18}$ cm^{-3} determined in the same paper.

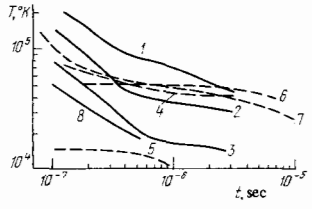

FIG. 17. Time variation of a laser-spark plasma temperature. 1–H_2, 4 atm [148]; 2–H_2, 8 atm [148]; 3–H_2, 6 atm [151]; 4–He, 4 atm [150]; 5–He, 10 atm [155]; 6–He, 0.75 atm [153]; 7–He, 0.5 atm [183]; 8–Xe, 1.4 atm [100].

Direct measurements of the concentration of the atoms in a laser-spark plasma in hydrogen was carried out by Evtushenko et al.[151] The concentration of the excited hydrogen atoms was determined from the H_α absorption line. The concentration of the normal atoms was calculated from the Boltzmann formula for the temperatures measured in the same study.

The results obtained in[151] have made it possible to trace the time variation of the mass density $\rho = m_H (n_e + n_a)$ (m_H is the hydrogen-atom mass) and of the pressure $p = kT(n_a + 2n_e)$ in the central regions of the laser spark. Figure 18 shows data on the time variation of the density, pressure, and temperature of the plasma. In the stage from 5×10^{-8} to 5×10^{-7} sec, plots of log (ρ/ρ_0), log (p/p_0) and log T (ρ_0 and p_0 are the initial density and pressure of the gas) against log t can be approximated by straight lines with slopes −1.3, −2.1, and −0.85. If it is assumed that the density vary in inverse proportion to the volume occupied by the shock wave, $\rho \sim V^{-1}$, that the adiabaticity condition $pV^\gamma = \text{const}$ is satisfied, and that the radius of the shock wave varies like $t^{2/5}$ in accordance with the theory of a point-concentrated explosion, then, as can be easily shown, the plasma parameters should vary like $\rho \sim t^{-6/5}$, $p \sim t^{-6\gamma/6}$ and $T \sim p/\rho \sim t^{-(6/5)(\gamma-1)}$. Putting $\gamma = 5/3$, we obtain $\rho \sim t^{-1,2}$, $p \sim t^{-2}$ and $T \sim t^{-0,8}$, which is in good agreement with the slopes of the experimental plots.

In the later stages (from 5×10^{-7} to 3×10^{-6} sec), the plasma parameter change very slowly. The pressure at the center is then close to the initial pressure. Such a relative stabilization of the plasma parameters can be attributed to the fact that the gas ceases to expand near the center when the pressure in the central region is equal to the external pressure. According to the theory of the point-concentrated explosion with allowance for counter pressure[132], the pressure of the gas at the center of the explosion practically ceases to vary at times $\tau \approx 0.2\,\tau_0$, where τ_0 is the dynamic time defined by the relation

$$\tau_0 = E_0^{1/3} \rho_0^{1/2} p_0^{-5/6}. \qquad (25)$$

The experimental conditions of[152] (spark in hydrogen

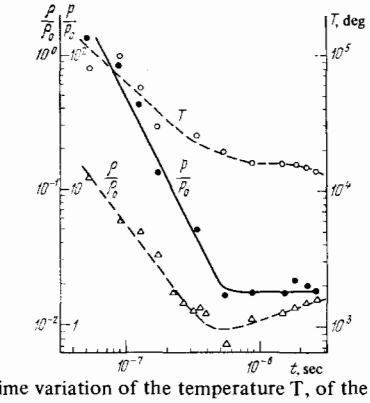

FIG. 18. Time variation of the temperature T, of the mass density ρ, and of the pressure p in a laser-spark plasma in hydrogen (ρ_0 and p_0 are the initial density and pressure of the gas) [151].

at 6 atm pressure) correspond to values $\rho_0 = 5.4 \times 10^{-4}$ g/cm^3, $p_0 = 6 \times 10^6$ dyn/cm^2, and $E_0 \approx 10^6$ erg (laser pulse energy 0.5 J; however, in accordance with the results of[135,136], only 20–25% of the laser-pulse energy is consumed in formation of the shock wave; see Fig. 13). Substituting these data in (25) we obtain $\tau_0 = 5 \times 10^{-6}$ sec and $\tau = 10^{-6}$ sec, which is close enough to the observed time of pressure stabilization.

The decrease of pressure in the center of the spark was observed in[148] up to a time $\approx \tau_0$, and it decreased to values much lower than p_0. This is probably due to insufficient allowance for the contribution made to the total pressure by the partial pressure of the atoms.

5. APPLIED RESEARCH

a) Production of high-temperature plasma. One of the most interesting trends in the investigation of the interaction between laser radiation and matter is the attempt to heat plasma to thermonuclear temperatures. Even though most papers devoted to this problem deal with the interaction of laser radiation with solid targets[1)] (see, e.g.,[156]), Pashinin and Prokhorov[157] have performed calculations according to which the use of breakdown in gas for this purpose may also be promising. The advantage of the gas medium is the possibility of working at plasma densities such that reflection of radiation from the plasma can be neglected, i.e., at $\nu > \nu_{pl}$ (ν is the radiation frequency and ν_{pl} is the plasma frequency). For radiation from ruby and neodymium lasers this condition leads to a plasma electron concentration $n_e \lesssim 10^{21}$ cm^{-3}.

The major obstacles to the attainment of high (thermonuclear) temperatures in gas breakdown by laser radiation (as well as interactions with solid targets) are the motion of the energy-release zone towards the laser and the hydrodynamic expansion of the plasma, as a result of which it is impossible to restrict the energy-release zone to the focal volume of the lens. Merely increasing the energy input is not sufficient to raise the plasma temperature appreciably, inasmuch as the volume from which the energy is released increases with increasing radiation intensity.

Thus, the problem of confining the plasma and localizing the energy-release volume comes to the forefront. To solve this problem, Pashinin and Prokhorov proposed to use a special gas target, a diagram of which is shown in Fig. 19. The plasma is produced inside a channel bounded by a bulky jacket covered on the ends by thin transparent films. The bulky jacket prevents radial expansion of the plasma. To decrease the energy losses due to the interaction of the plasma with the jacket, it is proposed to use a magnetic field parallel to the tube axis. According to the numerical estimates given in[157], to heat a mixture of deuterium with tritium at an initial pressure 20 atm in a tube 1.5 mm in diameter and 6 cm long to a temperature $\approx 10^8$ °K, and to obtain a positive thermonuclear-fusion energy yield it is necessary to have an energy $(3-5) \times 10^5$ J at a laser-pulse duration ≈ 70 nsec and a magnetic field $\approx 10^6$ Oe. These are realistically attainable values.

b) Interaction of laser-spark plasma with magnetic fields. There have been many attempts made to prevent the expansion of the laser spark by means of a magnetic field or by controlling other experimental conditions. The magnetic field needed to confine the plasma can be

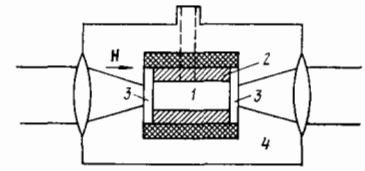

FIG. 19. Diagram of special gas target with magnetic field [157]. 1–channel with gas, 2–bulky tube, 3–windows, 4–vacuum chamber.

estimated from the condition that the magnetic pressure should exceed the gas-kinetic pressure of the plasma. This leads to the following relation between the field and the plasma parameters:

$$n_e kT < \frac{H^2}{8\pi}. \qquad (26)$$

Starting from this general condition, the value of the magnetic field was obtained in[158] for the case of a cylindrical plasma configuration with initial diameter 0.1 mm and length 1 mm at an initial deuterium-ion concentration 2×10^{21} cm^{-3} and $T = 10^7$ deg. It turned out to be approximately equal to 10^7 Oe.

Under real conditions, however, the laser-spark plasma temperature and the concentration of the electrons in it are much lower than the values assumed in these calculations, so that one can expect the action of weaker fields on the plasma.

Kaĭtmazov et al.[159] have shown that for the magnetic field to interact with the laser spark it is necessary, in addition to satisfying condition (26), to have the plasma dimensions exceed the skin-layer thickness. According to their calculations, fields lower than 3×10^5 Oe are practically incapable of acting on the laser spark under their experimental conditions. Accordingly, the investigations were carried out in a field 4×10^5 Oe. The laser spark in air was obtained by focusing neodymium-laser radiation of energy 2–3 J. When the direction of the field coincided with the direction of the laser beam, the spark had the form of a smooth line elongated along the field, rather than the bead-like structure observed in the absence of the field. On the other hand, when the direction of the field made an angle 45° with the direction of the laser beam, the spark was elongated not in the beam direction, as usual, but along the field direction.

Vardzigulova et al.[160] have observed that for a spark in air, at a pressure of 1 atm and lower, application of a magnetic field of 2×10^5 Oe leads to an increase of the time-integrated luminosity of the spark (the luminosity increased 1.4 times at p = 240 Torr). This is probably due to the slower expansion of the plasma in the magnetic field during the later stages of plasma development. They also observed a lowering of the breakdown threshold in the presence of a magnetic field, which is probably due to the decrease in the diffusion of the electrons from the focal region. It should be noted that Edwards and Litvak[161] did not observe a lowering of the breakdown threshold for a spark in argon in fields up to 10^5 Oe.

Chan et al.[162] investigated the influence of a magnetic field on a spark excited by a ruby laser in air, butane, and helium. The field applied by them ($H = 2 \times 10^5$ Oe) was, unlike in the earlier experiments, perpendicular to the direction of the laser beam. Under these conditions, no dependence of the breakdown threshold on the magnetic field was likewise observed, but a

clear-cut increase of the duration of the spark glow in the magnetic field was established.

Besides the influence of the magnetic field on the spark it was observed that the spark itself has, during the time it is acted upon by the laser radiation, a dipole magnetic moment perpendicular to the direction of the laser beam[163]. The magnetic moment appears in the case of asymmetrical passage of the laser beam through the lens, and its orientation is determined by the shift of the beam axis relative to the lens center.

Askar'yan et al.[164,165] investigated the diamagnetic perturbation of the external magnetic field by a laser spark. The spark was produced in a magnetic field (up to 10^4 Oe) parallel to the laser beam. An induction signal from a coil of 6 mm diameter, enclosing the spark, was measured. The observed diamagnetic perturbation of the external field was due to the propagation of the shock wave and persisted for a time interval larger by hundreds of times than the laser-pulse duration.

c) Certain methods of obtaining laser sparks. A number of methods were proposed to increase the efficiency with which the laser-spark plasma is heated. Thus, in[166], it was proposed to excite a laser spark by focusing the radiation on the front of a shock wave produced earlier by another auxiliary laser spark. The corresponding scheme is shown in Fig. 20. The axis of the laser beam producing the auxiliary laser spark is perpendicular to the plane of the figure. With such a geometry no laser spark is produced when the laser beam crosses for the first time the shock-wave front, because the light-flux density is low. The breakdown occurs on a shock-front surface remote from the focusing lens. A secondary shock wave is then produced. However, no energy is released from the front of this wave, which propagates in a direction opposite to the laser radiation, owing to the low gas density in the interior of the shock wave. Thus, the energy-release zone is localized near the focus of the lens. This should lead to an increase in the density of the energy absorbed near the focus and to a corresponding increase of the plasma temperature.

A number of original methods of obtaining a laser spark have been proposed by Askar'yan et al.[167,168]. In the first of these papers, it is proposed to focus the laser beam with a lens whose central part is covered by an opaque screen (Fig. 21). The spark produced by such a lens has a tubular geometry, and as a result of the "collapse" of the shock wave one can expect an appreciable increase in the temperature and pressure on the spark axis. In[168] a cylindrical lens was used for the focusing, and this made it possible to obtain a linear laser spark, which could be used to simulate linear explosions and cylindrical shock waves for ultrafast short-circuiting of high-voltage discharge gaps with large distances between electrodes. An extended spark can be obtained also by using the large spherical aberration of a conical lens. Such a scheme was used by Zel'dovich et al.[169]. In the case of focusing with a conical lens, the newly produced plasma foci do not block the access to the previously produced region thus resulting in a more uniform plasma heating than is attainable with spherical lenses. It is of interest to note that when an extended spark is produced the velocity of the breakdown front can be very high, even higher than the speed of light, since the development of the breakdown is determined by the character of the distribution of the field on the axis.

FIG. 20. Production of a laser spark by focusing laser radiation on the front of a shock wave [166]. 1—laser beam, 2—front of shock wave produced by auxiliary laser spark, 3—secondary shock wave.

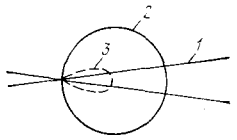

FIG. 21. Laser spark (3) produced by a lens (1) whose central part is covered by an opaque screen (2) [167].

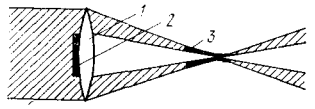

To obtain a laser spark, Mead[170] focused the beams of 12 synchronized lasers aimed at different angles onto one point of a gas-filled chamber. Such a scheme has made it possible to effect nearly-spherically-symmetrical plasma heating.

We mention also the work by Askar'yan and Tarasova[171], who investigated a laser spark in a small cloud of gas injected into a vacuum chamber through a rapid-action valve. They have proposed to use such a plasma to fill plasma traps.

A laser spark produced in a gas jet escaping from a high-pressure chamber into vacuum was investigated in[172,173]. The laser radiation was focused in a region of a strong gas-density gradient. The plasma boundary propagated in this case not towards the focusing lens but away from it, in the direction where the gas density increased[172]. This case is intermediate between a spark in a homogeneous gas and a plasma produced on the surface of a solid target.

d) Ignition of an electric discharge by a laser spark and other applications. A laser spark was used to ignite an electric discharge in many investigations. Most work on laser ignition of a spark gap were performed by focusing the laser radiation on the surface of one of the electrodes. A review of these investigations can be found in the paper by Guenther and Bettis[174].

Ignition of a discharge with the aid of a laser spark in gases was obtained by Vladimirov et al.[175]. Breakdown as a result of contact between a laser-spark plasma and electrodes occurs at voltages lower by 2—3 orders of magnitude than those required in the absence of the plasma. A laser spark makes it possible to synchronize conveniently the breakdown of the gap with other processes.

Koopman and Wilkerson[176] have observed the breakdown of a high-voltage gap (250 kV, 130 J) ignited by a long laser spark produced by a high-power neodymium laser. The stream of propagation was strictly along the laser spark.

Lowering of the breakdown voltage was observed in those cases when the density of the optical energy in the focus was insufficient to produce the spark. Thus, Akmanov et al.[177] ignited a low-voltage gap by focusing the radiation of the forward harmonic of a neodymium laser between the electrodes, and using intensities lower by two orders of magnitude than the optical-breakdown threshold.

Among other applications of the laser spark, notice should be taken of the possibility of using gas breakdown as an optical shutter that limits the peak power of a laser pulse passnig through it[178]. If the power of the input pulse exceeds the breakdown threshold, then breakdown takes place in the gas-filled chamber in which the

radiation is focused, and the remainder of the pulse is observed in the produced plasma. Passage of laser radiation through such a shutter can be used also to reduce the duration of a laser pulse. Such a shortened pulse was used, in particular, in[96,97] for optical diagnostics of a laser spark, and also in[54] to investigate the dependence of the breakdown threshold of CO_2-laser radiation on the duration of the laser pulse.

It should also be noted that the large brightness of the laser spark makes it possible to employ it as a light source to observe absorption spectra[151,179,180], and the high temperature at the initial stages of spark development makes it possible to excite with its aid a continuous spectrum as well as the spectra of highly-ionized atoms extending far into the region of the vacuum ultraviolet[181,182].

Notice should also be taken of the possibility of using a laser spark for the spectral analysis of the gases sealed in evacuated glass bulbs, without the need for breaking the seal.

The laser spark, which was discovered only ten years ago, has attracted, owing to its highly unique properties, much attention by researchers and is at present investigated perhaps no less than the usual spark discharge, which has been studied for approximately 100 years. One can assume that in the future the laser spark will find extensive application not only in physical research, but also in many technical applications.

Supplement. A large number of papers devoted to the laser spark were published while this review was being readied for press. Some of them are cited in the supplementary bibliography.

Theoretical and experimental investigations of the principal breakdown mechanisms, namely multiphoton and cascade ionization, are reported in[185]. A large group of papers[168] deals with breakdown of gases by CO_2-laser radiation.

The development of the laser spark during the time that the laser radiation acts on it is treated in[187,188]; most investigations have been devoted to laser sparks produced by CO_2 lasers operated either in the pulsed or stationary regime. An experimental observation of Compton scattering of laser radiation in a laser-spark plasma is reported in[188].

The development of a laser spark after the end of a laser pulse and the determination of the plasma parameters during the later stages of its development are the subject of[189]. Later papers are devoted to the possible use of a laser spark to obtain thermonuclear temperatures[190] and to initiate electric breakdown in a prescribed direction[199].

[1)] A review of the research on the interaction of laser radiation with solid targets was published by de Michelis [184].

[1] P. D. Maker, R. W. Terhune and C. M. Savage, Proc. of the 3rd Intern. Quantum Electronics Conference, Paris, 1963.
[2] Yu. P. Raĭzer, Usp. Fiz. Nauk 87, 29 (1965) [Sov. Phys.-Uspekhi 8, 650 (1966)].
[3] C. De Michelis, IEEE J. Quantum Electron. QE-5, 188 (1969).
[4] L. V. Keldysh, Zh. Eksp. Teor. Fiz. 47, 1945 (1964) [Sov. Phys.-JETP 20, 1307 (1965)].
[5] F. V. Bunkin and A. M. Prokhorov, ibid. 46, 1090 (1964) [19, 739 (1964)].
[6] P. Nelson, C. R. Ac. Sci. 259, 2185 (1964); 261, 3089 (1965).
[7] A. H. Gold and H. B. Bebb, Phys. Rev. Lett. 14, 60 (1965).
[8] H. B. Bebb and A. H. Gold, Phys. Rev. 143, 1 (1966).
[9] B. A. Tozer, ibid. A137, 1665 (1965).
[10] V. M. Morton, Proc. Phys. Soc. 92, 301 (1967).
[11] Y. Gontier and M. Frahin, C. R. Ac. Sci. B264, 499 (1967).
[12] L. P. Kotova and M. V. Terent'ev, Zh. Eksp. Teor. Fiz. 52, 732 (1967) [Sov. Phys.-JETP 25, 481 (1967)].
[13] E. R. Peressini, in: Physics and Quantum Electronics, ed. by P. L. Kelley, B. Lax, and P. E. Tannenwald, McGraw, 1966.
[14] A. M. Perelomov, V. S. Popov, and M. V. Terent'ev, Zh. Eksp. Teor. Fiz. 50, 1393; 51, 309 (1966); 52, 514 (1967) [Sov. Phys.-JETP 23, 924 (1966); 24, 207 (1967); 25, 336 (1967)].
[15] S. L. Chin, Canad. J. Phys. 48, 1314 (1970).
[16] G. S. Voronov, G. A. Delone, N. B. Delone, and O. V. Kudrevatova, ZhETF Pis. Red. 2, 377 (1965) [JETP Lett. 2, 237 (1965)].
[17] G. S. Voronov, G. A. Delone, and N. B. Delone, Zh. Eksp. Teor. Fiz. 51, 1660 (1966) [Sov. Phys.-JETP 24, 1122 (1967)].
[18] G. S. Voronov and N. B. Delone, ibid. 50, 78 (1966) [23, 54 (1966)].
[19] G. A. Delone and N. B. Delone, ibid. 54, 1067 (1968) [Sov. Phys.-JETP 27, 570 (1968)].
[20] P. Agostini, J. F. Bonnal, G. Mainfray and C. Manus, C. R. Ac. Sci. B266, 1034 (1968).
[21] P. Agostini, G. Barjot, G. Mainfray and C. Manus, ibid. A31, 367 (1970).
[22] G. Baravian, R. Benattar, J. Bretagne, J. L. Godart, and G. Sultan, Appl. Phys. Lett. 16, 162 (1970).
[23] G. A. Delone, N. B. Delone, N. P. Donskaya, and K. B. Petrosyan, ZhETF Pis. Red. 9, 103 (1969) [JETP Lett. 9, 59 (1969)].
[24] G. S. Voronov, Zh. Eksp. Teor. Fiz. 51, 1496 (1966) [Sov. Phys.-JETP 24, 1009 (1967)].
[25] Ya. B. Zel'dovich and Yu. P. Raĭzer, Zh. Eksp. Teor. Fiz. 47, 1150 (1964) [Sov. Phys.-JETP 20, 772 (1965)].
[26] J. R. Wright, Proc. Phys. Soc. 84, 41 (1964).
[27] D. D. Ryutov, Zh. Eksp. Teor. Fiz. 47, 2194 (1964) [Sov. Phys.-JETP 20, 1472 (1965)].
[28] G. A. Askar'yan and M. S. Rabinovich, Zh. Eksp. Teor. Fiz. 48, 290 (1965) [Sov. Phys.-JETP 21, 190 (1965)].
[29] V. A. Barynin and R. V. Khokhlov, Zh. Eksp. Teor. Fiz. 50, 472 (1966) [Sov. Phys.-JETP 23, 314 (1966)].
[30] A. V. Phelps, see ref.[13], p. 538 (see also ref.[8]).
[31] M. Young and M. Hercher, J. Appl. Phys. 38, 4393 (1967).
[32] Yu. V. Afanas'ev, É. M. Belenov, and O. N. Krokhin, ZhETF Pis. Red. 8, 209 (1968) [JETP Lett. 8, 126 (1968)].
[33] Yu. V. Afanas'ev, É. M. Belenov, and O. N. Krokhin, Zh. Eksp. Teor. Fiz. 56, 256 (1969) [Sov. Phys.-JETP 29, 141 (1969)].
[34] Yu. V. Afanas'ev, É. M. Belenov, O. N. Krokhin, and I. A. Poluéktov, ibid. 57, 580 (1969) [30, 318 (1970)].
[35] Yu. V. Afanas'ev, É. M. Belenov, I. A. Poluéktov, ZhETF Pis. Red. 15, 60 (1972) [JETP Lett. 15, 41 (1972)].
[36] R. W. Minck and W. G. Rado, see ref.[13], p. 527.
[37] F. Morgan, L. R. Evans and C. G. Morgan, J. Phys. D4, 225 (1971).

[38] R. W. Minck, J. Appl. Phys. **35**, 252 (1964).
[39] D. H. Gill and A. A. Dougal, Phys. Rev. Lett. **15**, 845 (1965) (see ref. [8]).
[40] A. F. Haught, R. G. Meyerand and D. C. Smith, see ref. [13], p. 509.
[41] R. G. Tomlinson, E. K. Damon and H. T. Buscher, ibid., p. 520 (see ref. [8]).
[42] W. Holzer, P. Ranson and P. Peretti, IEEE J. Quantum Electron. **QE-7**, 204 (1971).
[43] T. Bergqvist and B. Kleman, Ark. Fys. **31**, 177 (1966).
[44] M. Young, C. L. Chin and N. R. Isenor, Canad. J. Phys. **46**, 1537 (1968).
[45] D. C. Smith and A. F. Haught, Phys. Rev. Lett. **16**, 1085 (1966).
[46] B. F. Mul'chenko and Yu. P. Raĭzer, Zh. Eksp. Teor. Fiz. **60**, 643 (1971) [Sov. Phys.-JETP **33**, 349 (1971)].
[47] S. A. Akhmanov, A. I. Kovrigin, M. M. Strukov, and R. V. Khokhlov, ZhETF Pis. Red. **1**, No. 1, 42 (1965) [JETP Lett. **1**, 25 (1965)].
[48] H. T. Buscher, R. G. Tomlinson and E. K. Damon, Phys. Rev. Lett. **15**, 847 (1965) (see ref. [8]).
[49] C. Barthelemy, M. Leblanc and M. T. Boucalt, C. R. Ac. Sci. **B266**, 1234 (1968).
[50] A. J. Alcock, C. De Michelis and M. C. Richardson, Appl. Phys. Lett. **15**, 72 (1969).
[51] V. I. Eremin, L. V. Norinskiĭ, and V. A. Pryadin, ZhETF Pis. Red. **13**, 433 (1971) [JETP Lett. **13**, 307 (1971)].
[52] N. A. Generalov, V. P. Zimakov, G. I. Kozlov, V. A. Masyukov, and Yu. P. Raĭzer, ibid. **11**, 343 (1970) [JETP Lett. **11**, 228 (1970)].
[53] D. S. Smith, J. Appl. Phys. **41**, 4501 (1970).
[54] D. S. Smith, Appl. Phys. Lett. **19**, 405 (1971).
[55] V. E. Mitsuk, V. I. Savoskin, and V. A. Chernikov, ZhETF Pis. Red. **4**, 129 (1966) [JETP Lett. **4**, 88 (1966)].
[56] V. E. Mitsuk and V. A. Chernikov, ibid. **6**, 627 (1967) [JETP Lett. **6**, 124 (1967)].
[57] G. M. Barkhudarova, G. S. Voronov, V. M. Gorbunov, and N. B. Delone, Zh. Eksp. Teor. Fiz. **49**, 386 (1965) [Sov. Phys.-JETP **22**, 269 (1966)].
[58] D. S. Smith and R. G. Tomlinson, Appl. Phys. Lett. **11**, 73 (1967).
[59] A. J. Alcock, C. De Michelis and M. C. Richardson, IEEE J. Quantum Electron. **QE-6**, 622 (1970).
[60] C. C. Wang and L. J. Davis, Phys. Rev. Lett. **26**, 822 (1971).
[61] F. V. Bunkin and A. M. Prokhorov, Zh. Eksp. Teor. Fiz. **52**, 1610 (1967) [Sov. Phys.-JETP **25**, 1072 (1967)].
[62] A. J. Alcock, C. De Michelis and M. C. Richardson, Phys. Lett. **A28**, 356 (1968).
[63] A. J. Alcock and C. De Michelis, Phys. Rev. Lett. **21**, 667 (1968).
[64] C. De Michelis, Opt. Comm. **2**, 255 (1970).
[65] F. V. Bunkin, I. K. Krasyuk, V. M. Barchenko, P. P. Pashinin, and A. M. Prokhorov, Zh. Eksp. Teor. Fiz. **60**, 1326 (1971) [Sov. Phys.-JETP **33**, 717 (1971)].
[66] I. K. Krasyuk, P. P. Pashinin, and A. M. Prokhorov, ZhETF Pis. Red. **9**, 581 (1969) [JETP Lett. **9**, 354 (1969)].
[67] I. K. Krasyuk, P. P. Pashinin, and A. M. Prokhorov, Zh. Eksp. Teor. Fiz. **58**, 1606 (1970) [Sov. Phys.-JETP **31**, 860 (1970)].
[68] S. A. Ramsden and W. E. Davies, Phys. Rev. Lett. **13**, 227 (1964).
[69] S. A. Ramsden and P. Savic, Nature **203**, 1217 (1964).
[70] Yu. P. Raĭzer, Zh. Eksp. Teor. Fiz. **48**, 1508 (1965) [Sov. Phys.-JETP **21**, 1009 (1965)].
[71] J. W. Daiber and H. M. Thompson, Phys. Fluids **10**, 1162 (1967).
[72] Yu. P. Raĭzer, ZhETF Pis. Red. **7**, 73 (1968) [JETP Lett. **7**, 55 (1968)].
[73] J. L. Champetier, C. R. Ac. Sci. **261**, 3954 (1965).
[74] J. L. Champetier, M. Conairon and Y. Vendenboomgaerde, ibid., **B267**, 1133 (1968).
[75] R. E. Kidder, Nucl. Fusion **8**, 3 (1968).
[76] R. V. Ambartsumyan, N. G. Basov, V. A. Boiko, V. S. Zuev, O. N. Krokhin, P. G. Kryukov, Yu. V. Senatskiĭ, and Yu. Yu. Stoĭlov, Zh. Eksp. Teor. Fiz. **48**, 1583 (1965) [Sov. Phys.-JETP **21**, 1061 (1965)].
[77] A. J. Alcock, C. De Michelis, K. Hamal and B. A. Tozer, IEEE J. Quantum Electron. **QE-4**, 593 (1968).
[78] A. J. Alcock, C. De Michelis, K. Hamal and B. A. Tozer, Phys. Rev. Lett. **20**, 1095 (1968).
[79] C. Canto, J. D. Reuss and P. Veyrie, C. R. Ac. Sci. **B267**, 878 (1968).
[80] H. Hora, Phys. Fluids **12**, 182 (1969).
[81] H. Hora, Opto-Electronics **2**, 201 (1970).
[82] J. D. Lindl and P. K. Kaw, Phys. Fluids **14**, 371 (1971).
[83] S. L. Mandel'shtam, P. P. Pashinin, A. M. Prokhorov, Yu. P. Raĭzer and N. K. Sukhodrev, Zh. Eksp. Teor. Fiz. **49**, 127 (1965) [Sov. Phys.-JETP **22**, 91 (1966)].
[84] F. Floux and P. Veyrie, C. R. Ac. Sci. **261**, 3771 (1965).
[85] I. I. Komissarova, G. V. Ostrovskaya, and L. L. Shapiro, Zh. Tekh. Fiz. **40**, 1072 (1970) [Sov. Phys.-Tech. Phys. **15**, 827 (1970)].
[86] A. B. Ignatov, I. I. Komissarova, G. V. Ostrovskaya, and L. L. Shapiro, ibid. **41**, 701 (1971) [**16**, 550 (1971)].
[87] F. Floux, D. Guyot and P. Langer, C. R. Ac. Sci. **B267**, 416 (1968).
[88] J. L. Bobin, C. Canto, F. Floux, D. Guyot, and J. Reuss, IEEE J. Quantum Electron. **QE-4**, 923 (1968).
[89] N. G. Basov, V. A. Boiko, O. N. Krokhin, and G. V. Sklizkov, Dokl. Akad. Nauk SSSR **173**, 538 (1967) [Sov. Phys.-Dokl. **12**, 248 (1967)].
[90] V. V. Korobkin, S. L. Mandel'shtam, P. P. Pashinin, A. V. Prokhindeev, A. M. Prokhorov, N. K. Sukhodrev, and M. Ya. Shchelev, Zh. Eksp. Teor. Fiz. **53**, 116 (1967) [Sov. Phys.-JETP **26**, 79 (1968)].
[91] J. W. Daiber and H. M. Thompson, J. Appl. Phys. **41**, 2043 (1970).
[92] A. J. Alcock, P. P. Pashinin and S. A. Ramsden, Phys. Rev. Lett. **17**, 528 (1966).
[93] M. P. Vanyukov, V. A. Venchikov, V. I. Isaenko, P. P. Pashinin, and A. M. Prokhorov, ZhETF Pis. Red. **7**, 321 (1968) [JETP Lett. **7**, 251 (1968)].
[94] A. J. Alcock, E. Panarella and S. A. Ramsden, Proc. of the 7th Intern. Conference on Phenomena in Ionized Gases, v. 3, Beograd, 1965, p. 224.
[95] G. V. Ostrovskaya and Yu. I. Ostrovskiĭ, ZhETF Pis. Red. **4**, 121 (1966) [JETP Lett. **4**, 83 (1966)].
[96] A. N. Zaidel', G. V. Ostrovskaya, Yu. I. Ostrovskii, and T. Ya. Chelidze, Zh. Tekh. Fiz. **36**, 2208 (1966) [Sov. Phys.-Tech. Phys. **11**, 1650 (1967)].
[97] A. Kakos, G. V. Ostrovskaya, Yu. J. Ostrovskiy, and A. N. Zaidel, Phys. Lett. **23**, 81 (1966).
[98] M. Hugenschmidt, C. R. Ac. Sci. **B271**, 757 (1970).
[99] M. Hugenschmidt and K. Vollrath, ibid. **B272**, 36 (1971).
[100] M. Hugenschmidt, Zs. angew. Phys. **30**, 350 (1971).
[101] B. Z. Gorbenko, Yu. A. Drozhbin, S. D. Kaitmazov, A. A. Medvedev, A. M. Prokhorov, and A. M. Tomlachev, Dokl. Akad. Nauk SSSR **187**, 772 (1969) [Sov. Phys.-Dokl. **14**, 764 (1970)].
[102] M. Gravel, W. J. Robertson, A. J. Alcock, K. Büchl, and M. C. Richardson, Appl. Phys. Lett. **18**, 75 (1971).

[103] R. G. Tomlinson, ibid., p. 149.
[104] R. W. MacPherson and M. Gravel, Opt. Comm. **4**, 160 (1971).
[105] F. B. Bunkin, V. I. Konov, A. M. Prokhorov, and V. B. Fedorov, ZhETF Pis. Red. **9**, 609 (1969) [JETP Lett. **9**, 371 (1969)].
[106] Yu. P. Raĭzer, ibid. 11, 195 (1970) [11, 120 (1970)].
[107] Yu. P. Raĭzer, Zh. Eksp. Teor. Fiz. **58**, 2127 (1970) [Sov. Phys.-JETP **31**, 1148 (1970)].
[108] Yu. P. Raĭzer, Usp. Fiz. Nauk **108**, 429 (1972) [Sov. Phys.-Uspekhi **15**, 688 (1973)].
[109] B. F. Mul'chenko, Yu. P. Raĭzer, and V. A. Epshtein, Zh. Eksp. Teor. Fiz. **59**, 1975 (1970) [Sov. Phys.-JETP **32**, 1069 (1971)].
[110] N. A. Generalov, V. P. Zimakov, G. I. Kozlov, V. A. Masyukov, and Yu. P. Raĭzer, ZhETF Pis. Red. **11**, 447 (1970) [JETP Lett. **11**, 302 (1970)].
[111] N. A. Generalov, V. P. Zimakov, G. I. Kozlov, V. A. Masyukov, and Yu. P. Raĭzer, Zh. Eksp. Teor. Fiz. **61**, 1434 (1971) [Sov. Phys.-JETP **34**, 763 (1972)].
[112] R. W. Minck, J. Appl. Phys. **37**, 355 (1966).
[113] N. Ahmad, B. C. Gale and M. H. Key, J. Phys. **B2**, 403 (1969).
[114] R. G. Tomlinson, IEEE J. Quantum Electron. **QE-5**, 591 (1969).
[115] M. M. Savchenko and V. K. Stepanov, ZhETF Pis. Red. 8, 458 (1968) [JETP Lett. 8, 281 (1968)].
[116] V. V. Korobkin and A. J. Alcock, Phys. Rev. Lett. **21**, 1433 (1968).
[117] J. R. Wilson, J. Phys. **D3**, 2007 (1970).
[118] A. J. Alcock, C. De Michelis, V. V. Korobkin, and M. C. Richardson, Appl. Phys. Lett. **14**, 145 (1969).
[119] M. Young, M. Hercher and Chung Yiu Wu, J. Appl. Phys. **37**, 4938 (1966).
[120] A. J. Alcock, C. De Michelis, V. V. Korobkin and M. C. Richardson, Phys. Lett. **A29**, 475 (1969).
[121] M. H. Key, D. A. Preston and T. P. Donaldson, J. Phys. **B3**, L88 (1970).
[122] M. C. Richardson and A. J. Alcock, Appl. Phys. Lett. **18**, 357 (1971).
[123] P. Belland, C. De Michelis and M. Mattioli, Opt. Comm. **4**, 50 (1971).
[124] Yu. P. Raĭzer, ZhETF Pis. Red. **4**, 124 (1966) [JETP Lett. **4**, 85 (1966)].
[125] G. A. Askar'yan and I. L. Chistyĭ, Zh. Eksp. Teor. Fiz. **58**, 133 (1970) [Sov. Phys.-JETP **31**, 76 (1970)].
[126] G. A. Askar'yan, ZhETF Pis. Red. **4**, 400 (1966) [JETP Lett. **4**, 270 (1966)].
[127] A. G. Litvak, Izv. vuzov (Radiofizika) 8, 1148 (1965); 9, 629, 675, 900 (1966).
[128] P. Kaw, Appl. Phys. Lett. **15**, 16 (1969).
[129] H. Hora, Zs. Phys. **226**, 156 (1969).
[130] A. J. Palmer, Phys. Fluids **14**, 2714 (1971).
[131] L. I. Sedov, Metody podobiya i razmernosti v mekhanike (Similarity and Dimensional Methods in Mechanics), Moscow, Nauka, 1967 [Academic, 1959].
[132] V. P. Korobeĭnikov, N. S. Mel'nikova, and E. V. Ryazanov, Teoriya tochechnogo vzryva (Theory of Detonation from a Point), Fizmatgiz, 1961.
[133] E. Panarella and P. Savic, Canad. J. Phys. **46**, 183 (1968).
[134] T. P. Evtushenko, G. M. Malyshev, G. V. Ostrovskaya, V. V. Semenov and T. Ya. Chelidze, Zh. Tekh. Fiz. **36**, 1115 (1966) [Sov. Phys.-Tech. Phys. **11**, 818 (1966)].
[135] K. Büchl, K. Hohla, R. Wienecke and S. Witkowski, Phys. Lett. **A26**, 248 (1968).
[136] K. Hohla, K. Büchl, R. Wienecke and S. Witkowski, Zs. Naturforsch. **24a**, 1244 (1969).
[137] Ya. B. Zel'dovich and Yu. P. Raĭzer, Fizika udarnykh voln i vysokotemperaturnykh gidrodinamicheskikh yavleniĭ (Physics of Shock Waves and of High Temperature Hydrodynamics Phenomena), Nauka, 1966 [Academic, 1966].
[138] Deĭstvie yadernogo oruzhiya (Effects of Nuclear Weapons) (Collected translations), 2d. ed., Voenizdat, 1965.
[139] T. P. Evtushenko, A. N. Zaĭdel', G. V. Ostrovskaya, Yu. I. Ostrovskiĭ, and T. Ya. Chelidze, in: Diagnostika plazmy (Plasma Diagnostics), Part 2, Moscow, Atomizdat, 1968, p. 43.
[140] G. A. Askar'yan, M. S. Rabinovich, M. M. Savchenko, and V. K. Stepanov, ZhETF Pis. Red. **5**, 150 (1967) [JETP Lett. **5**, 121 (1967)].
[141] G. A. Askar'yan, M. S. Rabinovich, M. M. Savchenko, and A. D. Smirnova, ibid. **1**, No. 6, 18 (1965) [JETP Lett. **1**, 162 (1965)].
[142] G. A. Askar'yan, M. S. Rabinovich, A. D. Smirnova, and V. B. Studenov, ibid. **2**, 503 [**2**, 314 (1965)].
[143] G. A. Askar'yan, M. S. Rabinovich, M. M. Savchenko, and V. K. Stepanov, ibid. **3**, 465 (1966) [**3**, 303 (1966)].
[144] A. J. Alcock and S. A. Ramsden, Appl. Phys. Lett. 8, 187 (1966).
[145] I. I. Komissarova, G. V. Ostrovskaya, and L. L. Shapiro, Zh. Tekh. Fiz. **38**, 1369 (1968) [Sov. Phys.-Tech. Phys. **13**, 1118 (1969)].
[146] A. H. Guenther, W. K. Pendleton, C. Smith, C. H. Skeen and S. Zivi, J. Opt. Soc. Am. **61**, 688 (1971).
[147] T. P. Evtushenko, A. N. Zaĭdel', G. V. Ostrovskaya, and T. Ya. Chelidze, Zh. Tekh. Fiz. **36**, 1506 (1966) [Sov. Phys.-Tech. Phys. **11**, 1126 (1967)].
[148] M. M. Litvak and D. F. Edwards, J. Appl. Phys. **37**, 4462 (1966).
[149] G. Baravian, J. Bretagne, J. L. Delacroix, J. Godart, and G. Sultan, C. R. Ac. Sci. **B267**, 639 (1968).
[150] N. Ahmad, B. C. Gale and M. H. Key, Proc. Roy. Soc. **A310**, 231 (1969).
[151] T. P. Evtushenko, V. Kh. Mkrtchyan, and G. V. Ostrovskaya, Zh. Tekh. Fiz. **41**, 2581 (1971) [Sov. Phys.-Tech. Phys. **16**, 2049 (1972)].
[152] D. Bize, T. Consoli, L. Slama, P. Stevenin, and M. Zynanski, C. R. Ac. Sci. **B264**, 1235 (1967).
[153] E. V. George, G. Bekefi, and B. Ya'akoby, Phys. Fluids **14**, 2708 (1971).
[154] S. L. Mandel'shtam, P. P. Pashinin, A. V. Prokhindeev, A. M. Prokhorov, and N. K. Sukhodrev, Zh. Eksp. Teor. Fiz. 47, 2003 (1964) [Sov. Phys.-JETP **20**, 1344 (1965)].
[155] G. Lampis and S. S. Brown, Phys. Fluids **11**, 1137 (1968).
[156] N. G. Basov and O. N. Krokhin, Vest. AN SSSR, No. 6, 55 (1970).
[157] P. P. Pashinin and A. M. Prokhorov, Zh. Eksp. Teor. Fiz. **60**, 1630 (1971) [Sov. Phys.-JETP **33**, 883 (1971)].
[158] P. I. Shkuropat and G. A. Shneerson, Zh. Tekh. Fiz. **37**, 1161 (1967) [Sov. Phys.-Tech. Phys. **12**, 838 (1967)].
[159] S. D. Kaĭtmazov, A. A. Medvedev, and A. M. Prokhorov, ZhETF Pis. Red. **14**, 314 (1971) [JETP Lett. **14**, 208 (1971)].
[160] L. E. Vardzigulova, S. D. Kaĭtmazov, and A. M. Prokhorov, ibid. 6, 799 (1967) [JETP Lett. **6**, 253 (1967)].
[161] D. F. Edwards and M. M. Litvak, Bull. Am. Phys. Soc. 10, 73 (1965).
[162] P. W. Chan, C. De Michelis and B. Kronast, Appl. Phys. Lett. **13**, 202 (1968).
[163] V. V. Korobkin and R. V. Serov, ZhETF Pis. Red. **4**, 103 (1966) [JETP Lett. **4**, 70 (1966)].

[164] G. A. Askar'yan and M. S. Rabinovich, Zh. Eksp. Teor. Fiz. **48**, 290 (1965) [Sov. Phys.-JETP **21**, 190 (1965)].
[165] G. A. Askar'yan, M. M. Savchenko, and V. K. Stepanov, Zh. Eksp. Teor. Fiz. **59**, 1133 (1970) [Sov. Phys.-JETP **32**, 617 (1971)].
[166] N. Ahmad and M. H. Key, Appl. Phys. Lett. **14**, 243 (1969).
[167] G. A. Askar'yan, ZhETF Pis. Red. **10**, 392 (1970) [JETP Lett. **10**, 250 (1970)].
[168] G. A. Askar'yan and V. K. Stepanov, Zh. Eksp. Teor. Fiz. **59**, 366 (1970) [Sov. Phys.-JETP **32**, 198 (1971)].
[169] B. Ya. Zel'dovich, B. F. Mul'chenko, and N. F. Pilipetskii, ibid. **58**, 794 (1970) [Sov. Phys.-JETP **31**, 425 (1970)].
[170] S. W. Mead, Phys. Fluids **13**, 1510 (1970).
[171] G. A. Askar'yan and N. M. Tarasova, ZhETF Pis. Red. **14**, 89 (1971) [JETP Lett. **14**, 58 (1971)].
[172] H. M. Thompson, R. G. Rehm and J. W. Daiber, J. Appl. Phys. **42**, 310 (1971).
[173] H. J. Neusser, H. Puell and W. Kaiser, Appl. Phys. Lett. **19**, 300 (1971).
[174] A. H. Guenther and J. R. Bettis, Proc. IEEE **59**, 689 (1971) (see ref. **59** (4), 277 (1971)).
[175] V. I. Vladimirov, G. M. Malyshev, G. T. Razdobarin, and V. V. Semenov, Zh. Tekh. Fiz. **37**, 1742 (1967); **38**, 2109 (1968); **39**, 906 (1969) [Sov. Phys.-Tech. Phys. **12**, 1277 (1968); **13**, 1694 (1969); **14**, 677 (1969)].
[176] D. W. Koopman and T. D. Wilkerson, J. Appl. Phys. **42**, 1883 (1971).
[177] A. G. Akmanov, L. A. Rivlin, and V. S. Shil'dyaev, ZhETF Pis. Red. **8**, 417 (1968) [JETP Lett. **8**, 258 (1968)].
[178] R. G. Tomlinson, J. Appl. Phys. **36**, 868 (1965).
[179] L. N. Kaporskiĭ and G. S. Musatova, Zh. Prik. Spektr. **8**, 681 (1968).
[180] T. P. Evtushenko and G. V. Ostrovskaya, Zh. Tekh. Fiz. **40**, 1067 (1970) [Sov. Phys.-Tech. Phys. **15**, 823 (1970)].
[181] B. C. Fawcett, A. H. Gabriel, F. E. Irons, N. I. Peacock and P. A. H. Saunders, Proc. Phys. Soc. **88**, 1051 (1966).
[182] S. Dumartin, B. Oksengorn and B. Vodar, J. Chim. Phys. **64**, 235 (1967).
[183] W. F. Braerman, C. R. Stumpfel and H. J. Kunze, J. Appl. Phys. **40**, 2549 (1969).
[184] C. De Michelis, IEEE J. Quantum Electron. **QE-6**, 630 (1970).
[185] R. G. Evans and P. C. Thonemann, Phys. Lett. **A38**, 398 (1972); J. Bakos, A. Kiss, L. Szabo, and M. Tendler, ibid. **A39**, 283; G. J. Pert, IEEE J. Quantum Electron. **QE-8**, 623 (1972); N. K. Berezhetskaya, N. B. Delone, and T. T. Urazbaev, ZhETF Pis. Red. **15**, 478 (1972) [JETP Lett. **15**, 337 (1972); I. K. Krasyuk and P. P. Pashinin, ibid. p. 471 [333]; I. I. Kantorovich, Zh. Prik. Spektr. **16**, 605 (1972); P. de Montgolfier, J. Phys. **D5**, 1438 (1972); M. Jaouen, G. Laplanche, and A. Rachman, Phys. Lett. **A43**, 101 (1973); R. Parzynski, ibid. p. 171.
[186] D. R. Cohn, W. Halverson, B. Lax and C. E. Chase, Phys. Rev. Lett. **29**, 1544 (1972); D. R. Cohn, C. E. Chase, W. Halverson, and B. Lax, Appl. Phys. Lett. **20**, 225 (1972); G. A. Hill, D. J. James and S. A. Ramsden, J. Phys. **D5**, L97 (1972); C. H. Chan, C. D. Moody, and W. B. McKnight, J. Appl. Phys. **44**, 1179 (1973); C. D. Moody, Appl. Phys. Lett. **22**, 31 (1973); A. M. Robinson, ibid., p. 33; R. T. Brown and D. C. Smith, ibid., p. 245.
[187] D. L. Franzen, ibid. **21**, 62 (1972); A. A. Offenberger, and N. H. Burnett, J. Appl. Phys. **43**, 4977 (1972); L. C. Marquet, R. J. Hall, and D. C. Lencioni, IEEE J. Quantum Electron. **QE-8**, 564 (1972); B. Steverding, J. Phys. **D5**, 1824 (1972); V. K. Koncharov, A. N. Loparev, and L. Ya. Min'ko, Zh. Eksp. Teor. Fiz. **62**, 2111 (1972) [Sov. Phys.-JETP **35**, 1102 (1972)]; D. C. Smith and M. C. Fowler, Appl. Phys. Lett. **22**, 500 (1973); J. D. Strachan, Phys. Lett. **A42**, 507 (1973); C. C. Want and L. I. Davis, Jr., Opt. Comm. **7**, 61 (1973); E. Gernits, V. E. Mintsuk, and V. A. Chernikov, Zh. Tekh. Fiz. **43**, 563 (1973) [Sov. Phys.-Tech. Phys. **18**, 356 (1973)].
[188] N. H. Burnett, R. D. Kerr, and A. A. Offenberger, Opt. Comm. **6**, 372 (1972); A. A. Offenberger and N. H. Burnett, Phys. Lett. **A42**, 427 (1973); I. K. Krasyuk, P. P. Pashinin, and A. M. Prokhorov, ZhETF Pis. Red. **12**, 439 (1973) [JETP Lett. **12**, 305 (1973)].
[189] G. M. Malyshev, G. T. Razdobarin, and V. V. Semenov, Zh. Tekh. Fiz. **42**, 1428 (1972) [Sov. Phys.-Tech. Phys. **15**, 1104 (1972)]; R. C. Richardson and N. R. Isenor, Opt. Comm. **5**, 394 (1972); A. A. Offenberger and R. D. Kerr, J. Appl. Phys. **43**, 354 (1972); B. Ahlborn, Phys. Lett. **A40**, 289 (1972); G. A. Askar'yan, S. D. Kaĭtmazov, and A. A. Medvedev, Zh. Eksp. Teor. Fiz. **62**, 918 (1972) [Sov. Phys.-JETP **35**, 487 (1972)].
[190] P. P. Pashinin and A. M. Prokhorov, ibid. p. 189. [101].
[191] L. V. Norinskiĭ, Kvant. élektronika, No. 5, 108 (1971) [Sov. J. Quant. Electr. **1**, 519 (1972)]; L. V. Norinskiĭ, V. A. Pryadin, and L. A. Rivlin, Zh. Eksp. Teor. Fiz. **63**, 1649 (1972) [Sov. Phys.-JETP **36**, 872 (1973)]; K. A. Saum and D. W. Koopman, Phys. Fluids **15**, 2077 (1972).

Translated by J. G. Adashko